5-2012

Statistical Analysis of the Stress-Energy Methodology Applied to Cushion Curve Determination

Kendalyn Paulin
Clemson University, kpaulin@clemson.edu

STATISTICAL ANALYSIS OF THE STRESS-ENERGY METHODOLOGY APPLIED TO CUSHION CURVE DETERMINATION

A Thesis
Presented to
The Graduate School of
Clemson University

In Partial Fulfillment
of the Requirements for the Degree of
Master of Science
Packaging Science

---

by
Kendalyn Paulin
May 2012

Accepted by:
Dr. Ronald Thomas, Committee Chair
Mr. Gregory Batt
Dr. Matthew Daum

ABSTRACT

The stress-energy method is a proposed enhancement to ASTM D1596 that reduces all drop height, thickness and static load combinations into a single equation that can be used to generate any reasonable cushion curve for a particular material. There remains a question as to how accurate the stress-energy method can predict acceleration values and whether it is statistically comparable to ASTM D1596. There are three phases to this research that attempt to determine the accuracy of the stress-energy method: gathering data using the stress-energy method and analyzing the goodness of fit of the stress-energy equation, predicting a cushion curve and observing the upper and lower bounds for a given drop height and thickness, and using ASTM D1596 to create a cushion curve with the same drop height and thickness and comparing it to the predicted cushion curve.

ACKNOWLEDGMENTS

I would like to thank the Packaging Science Department of Clemson University and Mr. Gregory Batt in particular for his constant support, guidance and encouragement. Thanks are also in order for Dr. Matthew Daum for his cross-country support and Mr. Shane Hutchings for fixing any troublesome equipment. I also would like to thank BASF-The Chemical Company and Nova Chemicals, Inc. for their materials.

TABLE OF CONTENTS

TABLE OF CONTENTS (CONTINUED)

LIST OF TABLES

LIST OF FIGURES

CHAPTER ONE

INTRODUCTION:

When designing a cushion system, a packaging engineer will consult a set of cushion curves for a particular material in order to determine the appropriate thickness and surface area needed to protect a product from being damaged. Cushion curves illustrate the expected acceleration of cushion impact for a given drop height and thickness over a range of static loads. A set of cushion curves for a particular material is generated by performing thousands of test drops over a limited range of thicknesses and drop heights as per ASTM D1596 (American Society for Testing and Materials, 2011). This method has been used for the past fifty years and is an industry standard for evaluating the energy absorbing properties of polymeric materials.

An alternative technique, called the stress-energy method, has been proposed as an enhancement to ASTM D1596 that uses a single equation to produce any reasonable cushion curve for a given material. This method significantly reduces the number of necessary test drops, thus reducing laboratory test time and material. Test drops are performed using the same procedure as ASTM D1596, however the manner in which the data is set up and evaluated reduces all drop height, thickness and static load combinations into an equation that is used to predict acceleration with the help of spreadsheet software. From this, cushion curves for any reasonable drop height and thickness can quickly be generated.

There has been a question regarding the accuracy of the stress-energy method and whether or not it is statistically comparable to ASTM D1596. The objective of this work

is to statistically evaluate the stress-energy method as an acceptable enhancement to ASTM D1596 by analyzing the goodness of fit of the stress-energy equation and by comparing predicted and actual cushion curves over a range of drop heights, thicknesses and materials. The reduction of necessary test time and material and the ability to digitize data in order to predict acceleration for a specific drop height and thickness is beneficial to the packaging community.

CHAPTER TWO

LITREATURE REVIEW:

Distribution Cycle Hazards:

When a product needs to be transported from its place of manufacture to the consumer, it may go through multiple forms of distribution including sea, rail and truck or a combination of such. The type and duration of the expected hazards has an impact on cushioning selection. The three most common hazards are vibration, compression and shock.

Vibration is an oscillation or motion about a fixed reference point and occurs in all transportation methods (Soroka 2002). Vibration is described through the vertical distance moved from the reference point (amplitude) and the number of oscillations per second (frequency) and each mode of transportation produces a particular level of the two. Vehicle vibration occurs from the natural frequencies of the load, the suspension system, the engine, tire imbalances, and the trailer style as the vehicle encounters disturbances in the road (Soroka 2002). Rail vibration occurs through contact with the tracks and plane vibrations are caused by the engine and turbulence.

The package can receive surface damage through scuffing and abrasion and may also shift and settle during transport, but the most critical damage occurs through resonance. Vibration resonance occurs when the forcing (input) frequency is the same as the natural frequency of the object, which causes amplification in the amplitude and thus increases the acceleration and deceleration the object experiences (Soroka 2002). This can affect not only the package system as whole, but specific parts of the system as well.

The energy being placed on the system can fatigue, flex or crack delicate items, settle loose protective fill, disturb pallet patterns, cause containers to collide with one another and unscrew threaded fasteners (Soroka 2002). When redesigning the product to eliminate critical resonance points is not an option, cushioning material is added in order to minimize vibrations.

Compression occurs primarily when products are stacked on one another either in storage or transportation. There are two types of compression that can cause damage: dynamic and static. Dynamic compression is a mass load undergoing acceleration, such as a stack of product being placed in the back of a truck. Static compression occurs when a load is placed on a product, such as pallet stacking in a warehouse. Since products are often stored for long periods of time in warehouses, the temperature and humidity can affect the container's structural properties. According to Soroka, when a change in relative humidity from 40% to 90% occurs, corrugated material may lose about 50% of its' stacking strength (2002). Since the strongest load-bearing ability of a container resides in the corners, if packages are not stacked uniformly or if they are strapped down inappropriately, there is a loss of stacking strength.

Containers are often designed with compression strength in mind but it is important to consider the number of containers that will be placed upon it and any extra pallet weight additions. When a number of containers are stacked, the compression forces experienced by the bottom container will be much higher than the subsequent upper containers. When being transported, due to vibration resonance, the top packages may experience an amplified acceleration and repetitive shock due to bouncing if not properly secured (Soroka 2002).

Shock is defined as “an impact, characterized by a sudden and substantial change in velocity” (Soroka 2002). During a distribution cycle, shock may occur from accidental drops during manual handling, drops and side impacts from chutes and conveyers, falls from pallet loads, impacts from potholes or curbs during vehicle transport, impacts when a package is tipped over, or from rail cart coupling (Soroka 2002). The number and severity of impacts depends on the product’s distribution cycle and the weight of the object. Lighter packages often result in drops from higher drop heights.

Past studies have found that the probability of a package being dropped form a height greater than 40 inches is minimal, cautionary labeling only has a minor effect on handling, there is little control over drop orientation for smaller packages and packages receive many drops from low heights with only about one drop from a greater height (Soroka 2002).

Cushion Foams:

Cushioning material is often used in order to combat the detrimental effects of vibration, compression and shock. The focus of this research is on the effect cushioning has on the impact resulting from shock. Any material that deflects under an applied load can be considered a cushion. Cushioning materials can include cellulose-based materials such as molded pulp, corrugated inserts, and cellulose wadding. These materials are economically desirable but the shock absorbing properties, resiliency and cleanliness are subpar and are highly subjective to humidity changes (Soroka 2002).

A popular cushioning choice for packaging engineers is the use of polymeric foam. These materials can be produced at a range of densities and resiliencies, have minimal corrosive properties, are less subjective to humidity changes and can be cut or

molded into desired shapes (Soroka 2002). Examples of polymeric foam include expanded polyethylene, expanded polypropylene, expanded polystyrene, and expanded polyurethane foam among others. According to Hanlon, "foamed plastic can be defined as an expanded resinous material with a cellular sponge-like structure usually made by the introduction and dispersion of a gas in molten resin and the subsequent setting or curing of the expanded mass" (Hanlon 1998).

Polymeric foam can be divided into either open-cell or closed-cell foams depending on the gas structure. In open-cell foams, the cells, or air pockets are connected whereas closed-cell foams have networks of cells that are not interconnected. Open-cell foams have "higher absorptive capacity for water and moisture, a higher permeability to gas and vapor, less effective insulation capabilities for either heat or electricity, and a better ability to absorb and damp sound" (Klempner 2004). Closed-cell foams have higher mechanical qualities and are often used by packaging engineers because they provide better cushioning properties (Lee 2007).

The amount of energy experienced by a cushion during an impact is related to the change in velocity, or Velocity Change (ΔV). This is equal to the area under the curve in an acceleration versus time graph, otherwise known as a shock pulse, Figure 1. If no cushioning is used, the duration of the shock pulse is very short and the acceleration is very large. When proper cushioning is used, the cushioning slows down the impact from a shock and the duration of the shock pulse becomes longer and the resulting acceleration decreases. The area under the curve, velocity change, remains the same (Soroka 2002).

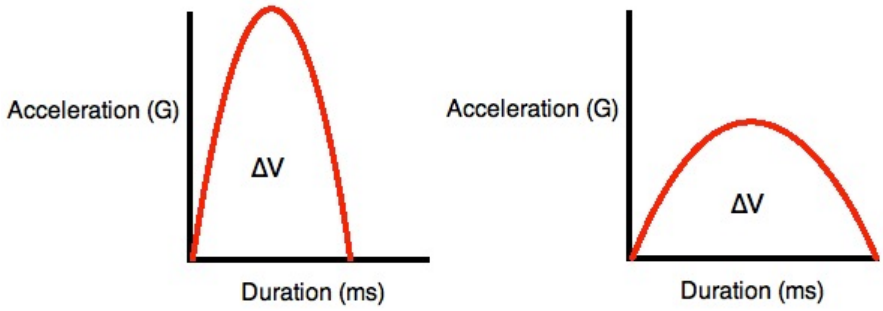

Figure 1: Example of a Shock Pulse Without and With Cushioning

If a cushion experiences an impact that involves a low weight over a large area, there is not enough force to deflect the cushion. This will result in a large acceleration since the cushion is not able slow down the impact. If the impact involves a large weight over a small area, the resulting acceleration will also be high. This is because the force of the impact is so great that the cushion is crushed beyond its' working length. The foam becomes so compacted that the effective stiffness increases.

Cushion Testing Using ASTM D1596:

ASTM D1596, "Standard Test Method for Dynamic Shock Cushioning Characteristics of Packaging Material" is the standard used in the packaging industry to determine the effectiveness of cushioning materials (ASTM). This standard was developed in 1956 and has been utilized for the past sixty years to create "Dynamic Cushion Curves". These curves are a way of graphically expressing the expected acceleration experienced by an expanded polymeric foam over a range of static loading for a given drop height and cushion thickness. Taking the weight of the product and dividing it by the load bearing surface area of the cushioning material in contact with the

product determines the static load. The cushion curves are plotted using acceleration versus static load and an example can be seen in Figure 2.

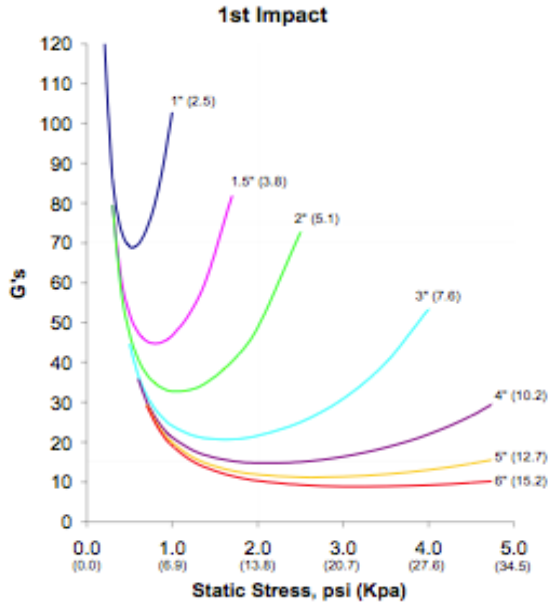

Figure 2: Cushion Curves for 1.3 lb/ft^3 ARCEL, Drop Height of 30 inches (Nova Chemical 2007)

Packaging engineers use cushion curves to determine the optimal thickness and area of cushioning they need in order to protect a product from damage. The drop height can be predicted by researching the common drop heights the package is likely to encounter during the distribution cycle. Another piece of information necessary in selecting the appropriate cushioning is the critical acceleration, which is the fragility of the product without any cushioning. The critical acceleration is the maximum change in acceleration that the product can survive. By understanding the expected drop height and critical acceleration, a packaging designer can then select the appropriate cushion thickness and static load. The goal of cushion curves is to prevent over-packing, which results in a waste of materials and space in the distribution cycle, while assuring protection of the product in its intended environment.

Even though cushion curves are a crucial packaging tool, using the ASTM D1596 method has certain drawbacks. To create a set of cushion curves with drops 1 through 5 for 7 static loads, 5 replicates, 5 thicknesses and 5 drop heights, one may have to perform over 4,375 drops. After completing a full set of cushion curves, the packaging engineer still has limited knowledge about the full performance of the cushioning material because the cushion curves are specific to only the drop heights and thicknesses tested. As seen in Figure 2, where curves are given for 2 and 3 inch material thickness, if one wants to know what the acceleration would be using a thickness of 2.5 inches, they would have to estimate or use a thicker material than necessary to prevent damage.

Stress-Energy Method:

Because of the extensive time and materials needed to create cushion curves that are limited to a certain range of thicknesses and drop heights, an enhancement to ASTM D1596 has been proposed. The stress-energy method was developed by Dr. Gary Burgess from Michigan State University in 1990 and was simplified by Dr. Matthew Daum over the following years. Burgess reasoned that cushioning data for a particular material could be consolidated into one stress-strain curve. He found that the amount of energy absorbed per unit volume of cushioning material is equal to the area under the stress-strain curve for that particular material. He claimed that the cushioning ability of a material is intrinsic to that particular material and that acceleration could be predicted for any drop height and thickness (Burgess 1990).

Burgess further reasoned that a new method could be used that would require less test drops by observing the amount of energy a cushion could absorb based on the

dynamic stress of that cushion. Dynamic stress, σ, can be predicted as some function of strain, ε, and strain rate $\frac{d\varepsilon}{dt}$, Equation 1.

$$\sigma = funct\left(\varepsilon, \frac{d\varepsilon}{dt}\right) \qquad \text{Equation 1}$$

Instead of testing a material using multiple samples and measuring the specific properties, the cushioning ability of the foam should be viewed as a property of the material as a whole. The stress-energy model plots dynamic stress, DS (Equation 2) versus dynamic energy, DE (Equation 3), where s is the static load, h is drop height, t is thickness and G is acceleration. An exponential curve is then fitted to the cushion test data (Equation 4). This equation is specific to a particular material, where y is dynamic stress, DS, x is dynamic energy, DE, and 'A' and 'B' are unitless coefficients found through curve fitting (Daum 2006).

$$DE = \frac{sh}{t} \qquad \text{Equation 2}$$

$$DS = Gs \qquad \text{Equation 3}$$

$$y = Ae^{Bx} \qquad \text{Equation 4}$$

Once the A and B constants are determined from the dynamic stress versus dynamic energy curve, Equation 4 can be rearranged to calculate acceleration for any drop height, thickness and static load combination, Equation 5.

$$G = \frac{Ae^{B\left(\frac{sh}{t}\right)}}{s} \qquad \text{Equation 5}$$

Using this equation, one can predict an acceleration value by inputting the desired static load, drop height and thickness without having to perform any further cushion testing. This allows for more precise drop height and thickness selections. By utilizing

spreadsheet software, a cushion curve can be generated by plotting a range of static loads and the resulting calculated accelerations. This curve can quickly be changed to reflect any desired thickness and drop height combination.

Marcondes et al of Clemson University performed further research using the stress-energy method on cushions ranging from one to three inches thick. This work determined that three different energy levels, with five samples at each level, is adequate to produce cushion curves (2008). These three energy levels are chosen based on the expected energy of the desired material and can be either estimated or determined through pre-testing. They often range from 10 to 50 in-lb/in^3 but can vary based on the distribution cycle. The third energy level should be selected at about halfway between the high and low energy values (Marcondes et al 2008). Using slope, intercept and a standard t-test, this work found that there was no statistical difference between linearized lines created with five energy levels and those created with three energy levels. This results in a further reduction of test time and materials (Marcondes et al 2008).

Glen Potter of Clemson University determined that the stress-energy method was not as accurate in predicting the accelerations of drops on cushions less than one inch thick unless the original stress-energy testing included samples that were less than one inch thick (Potter 2010).

Statistical Accuracy

There remains a question regarding the accuracy of the stress-energy method and its ability to predict a material's cushioning properties. Historically, the coefficient of

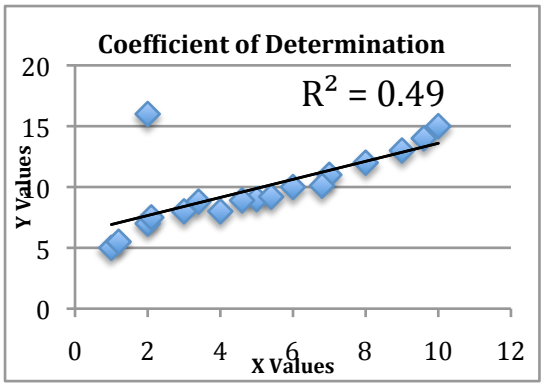

Figure 3: Data Set With r^2 Value

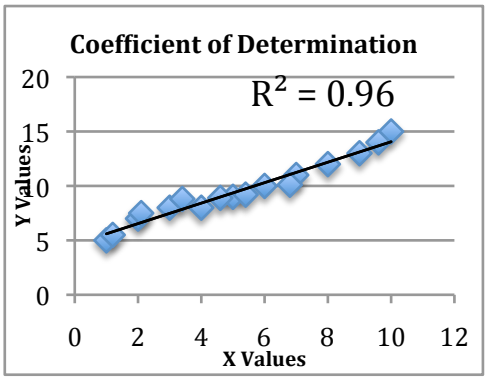

Figure 4: Data Set With r^2 Value With Outlier Removed

determination, or r^2 value, has been used to evaluate the goodness of fit of the stress-energy model, as has been the case with the stress-energy method to this point. The r^2 value, or coefficient of determinations, is a value ranging from 0 to 1 that described how well the model explains the variation of stress. A value of 1 means the x and y values are perfectly related and there is no residual variation and statisticians usually accept anything above a 0.90 as statistically acceptable. However, there is a limitation on solely relying on the r^2 value to determine the goodness of fit of a model. If there is an outlier in a set of data, it has the ability to push or pull the regression line in a particular direction, giving the false appearance of a trend. Figure 3 shows the graph of an arbitrary set of data and the r^2 generated using Microsoft Excel. Figure 4 shows the generated regression line and r^2 with the one outlier removed.

In order to compare actual acceleration values to those predicted by the stress-energy method, many different methods have been utilized. Previous work compared predicted deceleration values to actual recorded deceleration values for two materials and a range of thicknesses and found a 10% difference for 9.0 lb/ft^3 expanded polyethylene and a 12% difference for 1.25 lb/ft^3 expanded polystyrene (Daum 2011). Another study evaluated the proportion of deceleration values resulting in the same thickness as ASTM

D1596, within a range of standard thicknesses and determined that the stress-energy method yields greater variability than ASTM D1596 (Singh 2010). Singh's work determined that there was as high as a 27.5% difference for 1.7 lb/ft^3 expanded polyethylene (2010).

The goal of this research is to use regression analysis to determine the coefficient of determination, the sum of squared errors and root mean square error of the stress-energy equation for ten different data sets. The hope is that the root mean square error will be a more informative and descriptive method of determining goodness of fit in addition to the coefficient of determination. The next phase of this research is to use the stress-energy equation to determine the upper and lower bounds of a predicted cushion curve given the variability of the A and B constants. Then, in order to determine how well the stress-energy method can predict acceleration values, a range of cushion curves will be created using ASTM D1596 and compared to the predicted cushion curve at various combinations of drop heights and thicknesses. The scope of this research will be limited to analyzing the data from drops 1 and 2 because most package systems encounter two major impacts during the distribution cycle (Rabenhorst 2006).

CHAPTER THREE

MATERIALS AND METHODS:

Test Equipment:

The test equipment used for this research was a Lansmont Cushion Test model 23. A PCB piezoelectric accelerometer, model 353B15, sensitivity 10.42 mV/g, was mounted to the platen weight. The shock pulses were captured and analyzed with Lansmont Test Partner TP3 data acquisition software. The equivalent free fall drop height was calculated using Lansmont Test Partner Velocity Sensor software version 2.0.1. All equipment used was compliant with ASTM D1596. Figure 5 shows the equipment setup.

Figure 3: Lansmont Cushion Tester Model 23

The equivalent free fall drop height, h_{eq}, was calculated based on the impact velocity, V_i, which was measured just prior to impact with the cushion using Equation 6,

where g is the acceleration due to gravity. The equivalent free fall drop height is important because as the platen weight falls, it encounters friction from the guiderails that slows the platen down. The guide rails are necessary for the platen weight to fall flat and on target. The friction causes the actual measured drop height to be greater than the equivalent free fall drop height so velocity must be used to ensure the correct amount of energy is being input into the cushion system.

$$h_{eq} = \frac{V_i^2}{2g} \qquad \text{Equation 6}$$

When the platen falls onto the cushion, the accelerometer records a shock pulse that must be filtered using an electronic filter in order to remove any high frequency 'noise'. Figures 6 and 7 show a shock pulse before and after filtering. Equation 7 is used to determine the proper filtering frequency for each drop. The filter frequency, F_f, is a function of the duration of the shock pulse, τ_{10}. The duration is determined by selecting the rise and fall of the shock pulse that correlate to 10% of the peak acceleration.

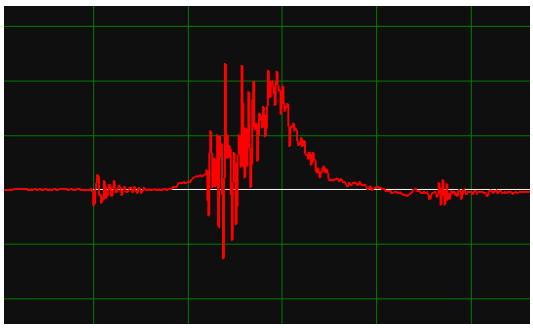

Figure 6: Shock Pulse Before Filtering

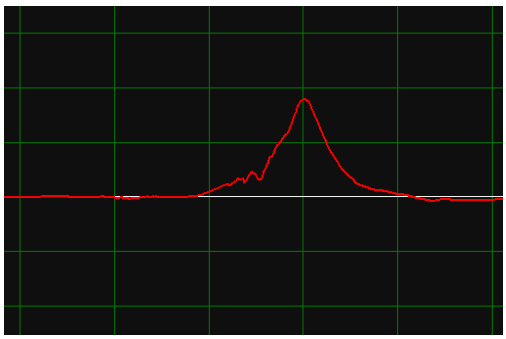

Figure 7: Shock Pulse After Filtering

$$F_f \geq 10\left(\frac{1}{2\tau_{10}}\right) \qquad \text{Equation 7}$$

Materials:

Five different densities of Material X were tested and analyzed using the stress-energy method (1.0 lb/ft^3, 1.25 lb/ft^3, 1.50 lb/ft^3, 1.75 lb/ft^3, 2.20 lb/ft^3). This material is an expanded polymer foam and the exact specifications are being withheld to protect the manufacturer. All sample prep and testing took place at the Sonoco Packaging Laboratory at Clemson University. For each density, preliminary testing for the maximum and minimum energy properties yielded a selection of four unique energy levels. Once these levels were determined, appropriate cushion samples were cut using a bandsaw and then stored in an environmental chamber at 73° F and 50% relative humidity for at least 24 hours. At each energy level, five combinations of static load, drop height and thickness were tested. Table 1 shows the energy levels and combinations used for Material X 1.00 lb/ft^3, and all five testing specifications for Material X can be found in Appendix A.

Table 1: Testing Specifications for Material X 1.00 lb/ft^3

Sample	Expected Energy	Area (in^2)	Weight (lbs)	Static Load (lb/in^2)	Drop Height (in)	Thickness (in)
1.0_1.1	15	16.00	13.73	0.86	17.50	1.00
1.0_1.2	15	16.00	20.00	1.25	12.00	1.00
1.0_1.3	15	16.00	20.00	1.25	18.00	1.50
1.0_1.4	15	16.00	32.66	2.04	14.70	2.00
1.0_E4	15	16.00	45.68	2.86	10.50	2.00
1.0_2.1	22	16.00	20.00	1.25	17.60	1.00
1.0_2.2	22	16.00	32.66	2.04	10.80	1.00
1.0_2.3	22	16.00	32.66	2.04	16.20	1.50
1.0_E3	22	16.00	45.68	2.86	11.60	1.50
1.0_2.5	22	16.00	32.66	2.04	21.50	2.00
1.0_3.1	29	16.00	32.66	2.04	14.20	1.00
1.0_3.2	29	16.00	45.68	2.86	15.70	1.50
1.0_3.3	29	16.00	32.66	2.04	21.30	1.50
1.0_3.4	29	16.00	45.68	2.86	20.20	2.00
1.0_3.5	29	16.00	32.66	2.04	28.50	2.00
1.0_E1	35	16.00	32.66	2.04	17.10	1.00
1.0_4.2	35	16.00	45.68	2.86	18.80	1.50
1.0_4.3	35	16.00	32.66	2.04	25.70	1.50
1.0_E5	35	16.00	45.68	2.86	24.50	2.00
1.0_4.5	35	16.00	51.95	3.25	21.50	2.00

The cushion testing was performed in accordance with ASTM D1596. Five drops were performed on each sample, allowing sixty seconds between each drop. Each shock pulse was filtered and analyzed and the peak acceleration was recorded. Using the resulting data, a stress-energy plot was created for drops 1 and 2 for each of the five densities. This was accomplished by plotting the Dynamic Stress versus Dynamic Energy using the statistical software, JMP version 9.0. Dynamic Energy was the drop height multiplied by the static load and divided by the thickness and Dynamic Stress was calculated by multiplying the peak acceleration by the corresponding static load. A fitted exponential line and equation were then added to the plot by using the software's regression capabilities.

The stress-energy equation of Drops 1 and 2 of the five densities of Material X were analyzed in addition to five other sets of data that had been previously tested using the stress-energy method at Clemson University. Material S 1.90 lb/ft^3, Material T 1.90 lb/ft^3, and three densities of Material U, 1.30 lb/ft^3, 1.50 lb/ft^3, and 1.90 lb/ft^3. All of these materials were comprised of an expanded polymer, including polyethylene, polystyrene or a copolymer of a similar nature. The stress-energy data from Drops 1 and 2 of each of these five data sets were also analyzed using JMP 9.0 using regression analysis. The ten data sets can be seen in Table 2 including the number of energy levels used.

Table 2: Stress-Energy Data Sets Used for Regression Analysis

Material	Energy Levels
S 1.90 lb/ft^3	3
T 1.90 lb/ft^3	3
U 1.30 lb/ft^3	3
U 1.50 lb/ft^3	3
U 1.90 lb/ft^3	3
X 1.00 lb/ft^3	4
X 1.25 lb/ft^3	4
X 1.50 lb/ft^3	4
X 1.75 lb/ft^3	4
X 2.20 lb/ft^3	4

In order to create cushion curves using the traditional ASTM D1596 method, Material X was chosen for cushion testing using a range of drop height and thickness combinations. All five densities were used, with one repeat, yielding a total of six cushion curve data sets, Table 3. Cushion samples were prepared as per ASTM standards with each cushion curve using five replicates at six or seven static loads. Five drops were performed on each sample with a minute in between each drop and peak accelerations were recorded. The accelerations of each of the five replicates at each static load were averaged together for both drop 1 and 2. Cushion curves for both drops were created by plotting the average acceleration versus static load.

Table 3: Cushion Curve Data Sets Using ASTM D1596

Cushion Curve Data Set Label	Material	Thickness (in)	Drop Height (in)
A	X 1.00 lb/ft^3	1.5	18
B	X 1.25 lb/ft^3	1.0	24
C	X 1.50 lb/ft^3	2.0	20
D	X 1.75 lb/ft^3	1.0	18
E	X 1.75 lb/ft^3	2.0	36
F	X 2.20 lb/ft^3	2.0	28

Data Treatment:

The purpose of this work was to determine how statistically accurate the stress-energy method was at predicting acceleration values. Specifically, how well these values compare to cushion curves produced using the traditional ASTM D1596 method at a range of drop height and thicknesses. In order to evaluate the stress-energy method, this work was divided into three phases.

Phase I. The first method was to analyze Drop 1 and 2 from the ten stress-energy data sets from Table 6 by performing regression analysis using JMP 9.0. This includes fitting an exponential line and equation to each data set and calculating the A and B constants as well as the standard error and the 95% confidence intervals of these two values. The sum of squared errors (SSE), root mean square error (RMSE), and the coefficient of determination (r^2) of the fitted exponential equation were also calculated using the statistical software.

Using JMP 9.0, the exponential equation, Equation 4, was applied to each of the ten data sets in order to determine the predicted stress given the Dynamic Energy found during testing, Figure 8. Temporary values of 1 are input for the constants A and B and

will be determined during analysis. The output and corresponding plot using the stress-energy data set Material X 1.75 lb/ft^3 can be seen in Figure 9. The upper and lower "CL" are the 95% confidence levels of the A and B parameters using an alpha of 0.05.

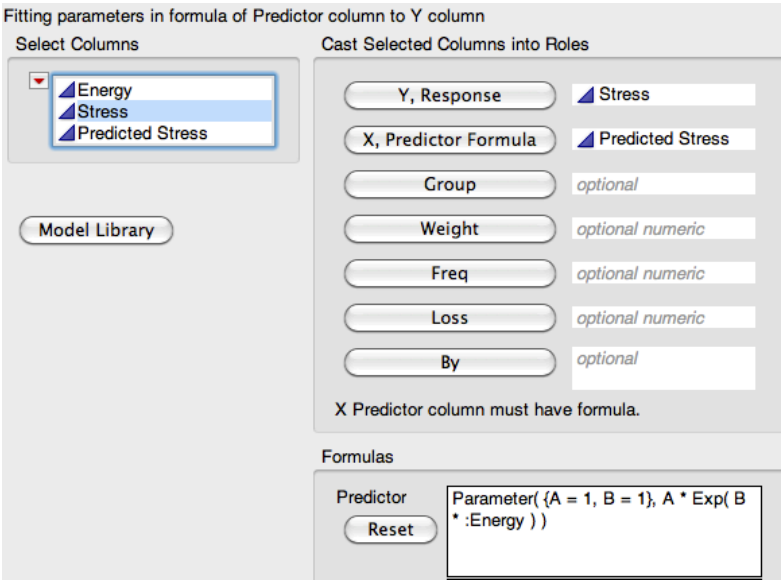

Figure 8: JMP Nonlinear Regression Analysis Setup

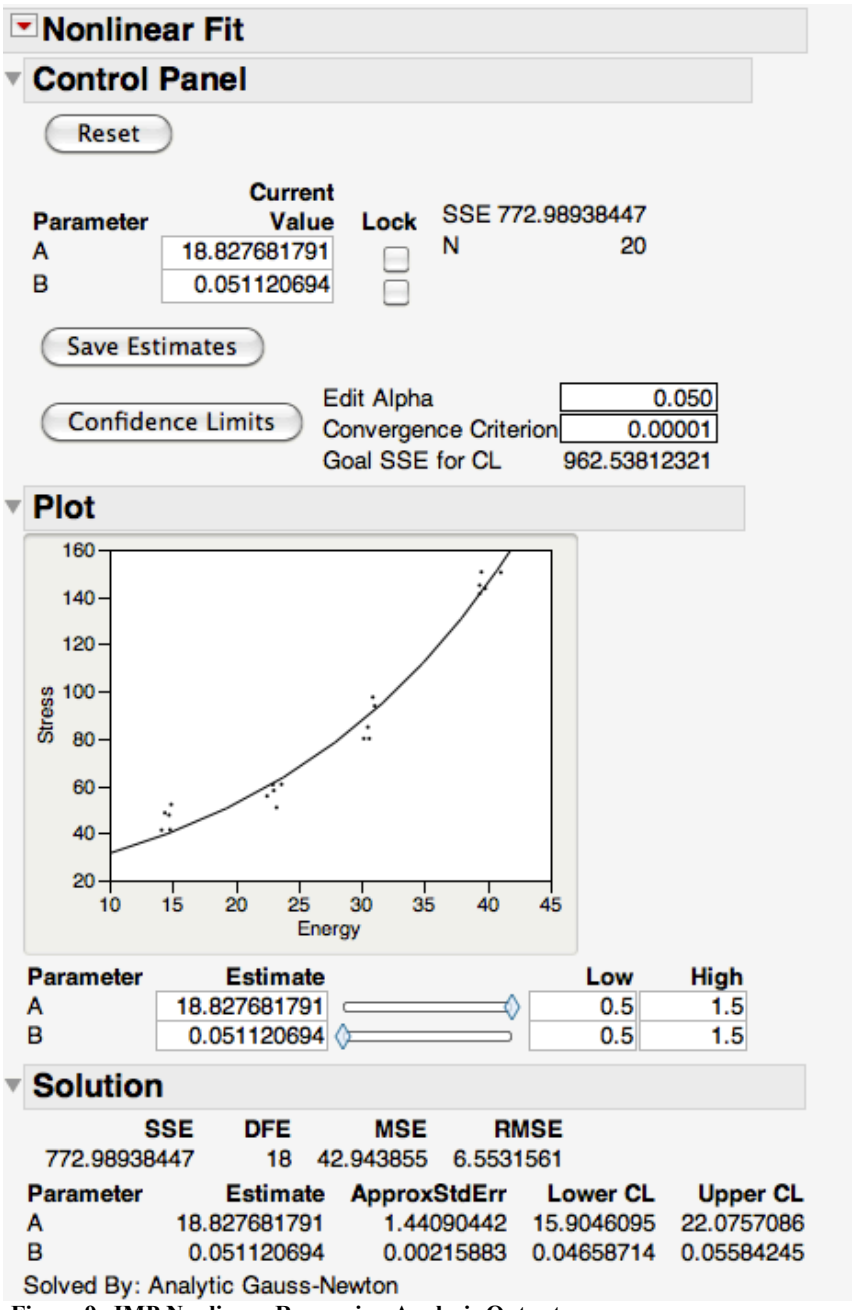

Figure 9: JMP Nonlinear Regression Analysis Output

The sum of squares of the errors represents the sum of the distance between each actual dynamic stress values (the data points) and their predicted dynamic stress values, which is the dynamic stress value of the regression line at the same dynamic energy, Equation 8. Squaring the distance removes any negative values.

$$SSE = \sum_{i=1}^{n} (y_i - \hat{y}_i)^2 \qquad \text{Equation 8}$$

The root mean square error is the square root of the sum of square error divided by the number of samples minus the number of unknown parameters, which is 2 since A and B are the two unknowns, Equation 9. It represents the distance, on average, of a data point from the fitted line, measured along the dynamic stress axis. Because this is the square root of a squared value, the units will be the same as the dynamic stress. The smaller the RMSE, the better the data points follow the regression line.

$$RMSE = \sqrt{\frac{\sum_{i=1}^{n} (y_i - \hat{y}_i)^2}{n - k}} \qquad \text{Equation 9}$$

The coefficient of determination, or r squared value, is a value that explains how well the model explains the variation in dynamic stress, Equation 10. A value of 1 represents a perfect correlation between Dynamic Stress and Dynamic Energy and a value of 0 means there is no correlation. Statisticians usually accept any value greater than 0.90 as statistically significant. An r^2 value could also be described in terms of a percentage, such as 90% of the data can be accurately explained using the regression model.

$$r^2 = 1 - \frac{\sum_{i=1}^{n} (y_i - \bar{y})^2}{SSE} \qquad \text{Equation 10}$$

Phase II. The second method of analysis was to use the upper and lower confidence levels of the A and B constants found in Figure 9 in order to create upper and lower stress-energy confidence bounds. By using equation 4 and replacing the A and B with the

respective upper and lower confidence levels, upper and lower bound stress-energy equations are determined for each stress-energy data set. Equation 11, 12, and 13 are the upper and lower stress-energy equations for Material X 1.75 lb/ft^3.

Stress-Energy Equation $y = 18.83e^{0.0511x}$ Equation 11

Lower Bound S-E Equation $y = 15.90e^{0.0466x}$ Equation 12

Upper Bound S-E Equation $y = 22.08e^{0.0558x}$ Equation 13

Once these respective equations are determined for each stress-energy data set, upper and lower cushion curve confidence bounds can be calculated for a given drop height and cushion thickness using Equation 5 from the simplified stress-energy method. Figure 10 shows the original, upper and lower cushion curves produced using Material X 1.75 lb/ft^3 and a drop height of 18 inches and a thickness of 1 inch. This represents with 95% confidence that the actual cushion curve generated using the calculated stress-energy equation will fall between the upper and lower confidence bounds.

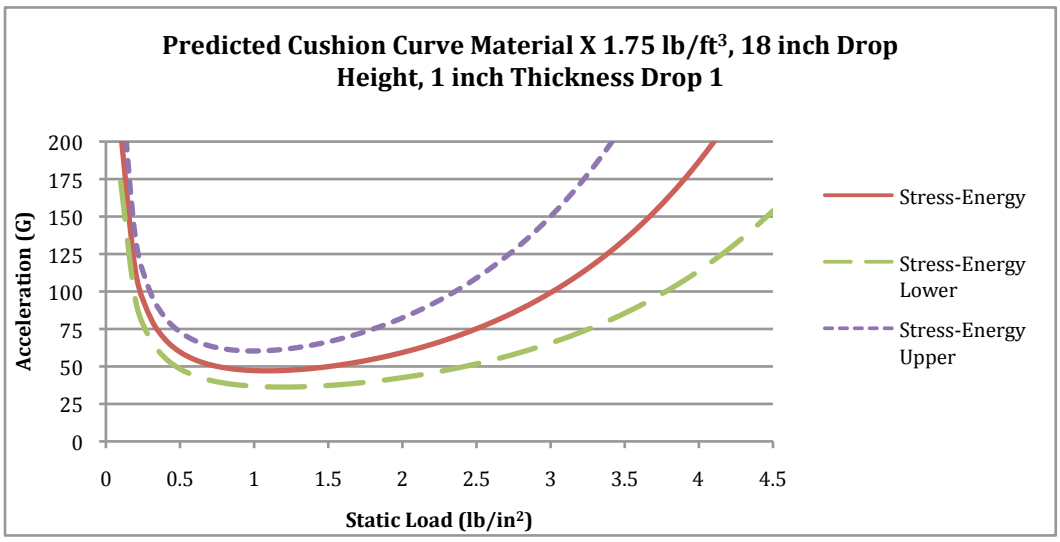

Figure 10: Predicted Cushion Curve Confidence Bounds

Phase III. The next analysis method was to use the traditional ASTM D1596 method to produce cushion curves at a range of drop heights and thicknesses and then compare them to the generated cushion curves found in Phase II. From this, the difference and percent difference between the actual and predicted accelerations were calculated using Equation 14 and 15, respectively, where Y_{ASTM} is the acceleration recorded using the traditional ASTM D1596 method and Y_{SE} is the acceleration predicted by the stress-energy generated cushion curve at the corresponding static load.

$$Difference = |Y_{SE} - Y_{ASTM}| \qquad \text{Equation 14}$$

$$\%Difference = \left|\frac{Y_{ASTM} - Y_{SE}}{Y_{ASTM}}\right| \times 100 \qquad \text{Equation 15}$$

In addition to calculating the difference and percent difference between the two acceleration values, the maximum and minimum acceleration allowed between laboratories by the precision and bias section of ASTM D1596 were also calculated, Equation 16, 17. ASTM D1596 states:

> "The between laboratory reproduction standard deviation for one type of elastomeric pad ranged from 5 to 15 g's, 9 to 18% of the mean. This depends on the type and loading of the cushion and on the type of equipment used by the laboratories" (2011).

$$Y_{+18\%Error} = Y_{ASTM} \times 1.18 \qquad \text{Equation 16}$$

$$Y_{-18\%Error} = Y_{ASTM} \times 0.82 \qquad \text{Equation 17}$$

CHAPTER FOUR

RESULTS AND DISCUSSION:

Phase I. The stress-energy data from Drop 1 and 2 for the five densities of Material X were plotted and a regression line was fitted using JMP 9.0. For all five data sets, as dynamic energy increases, dynamic stress increases in an exponential fashion, which is expected for stress-energy polymer foam performance. The data for Drop 1 for all five densities had lower dynamic stress values than Drop 2 for each dynamic energy level. The stress-energy data and regression line for Material X 1.00 lb/ft^3 for Drop 1 and 2 can be seen in Figure 11, and all five stress-energy graphs can be seen in Appendix B. The values for the Dynamic Stress axis have been removed for proprietary reasons.

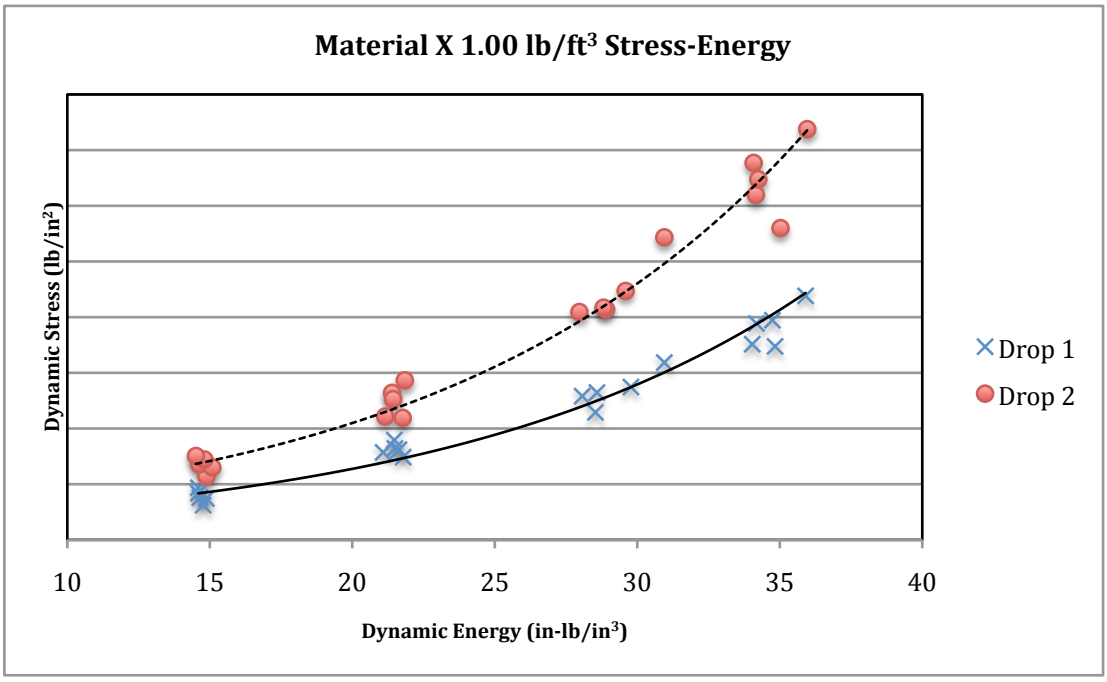

Figure 11: Stress-Energy Plot Material X 1.00 lb/ft^3

As Dynamic Energy increases, there appears to be an increase in variation, or the spread of the x axis values. This is commonly seen in stress-energy plots, especially those with high Dynamic Energy levels. In order to achieve high Dynamic Energy values, there is a physical limitation regarding the static load and thickness selection, thus drop height is the remaining variable that must be increased. At high drop heights, the cushion tester undergoes greater variation in performing consistent velocities due to the friction of the guiderails. This causes a greater variation in the actual Dynamic Energy. However, the variation is not a concern because even though these Dynamic Energy values may not be the same as the desired energy levels, the regression analysis takes every data point into account. Using the traditional ASTM D1596 cushion curve method, variation in recorded drop height, which is typically seen at greater drop heights, is not taken into account when plotting acceleration versus static load. This leads one to believe that every drop was performed at the exact drop height, which is difficult to achieve at higher drop heights. For example, during testing at 36 inches, the highest recorded drop height was 37.75 inches and the lowest was 35.01 inches. The stress-energy method uses the actual recorded drop heights and the variation is utilized in the regression analysis.

All ten stress-energy data sets where analyzed using JMP 9.0 to determine the respective A and B constants of the stress-energy equation for Drop 1 and 2, as well as the standard error and upper and lower 95% confidence limits, Tables 4 and 5. The sum of squared errors, root mean square error, and the coefficient of determination (r^2) were also calculated for Drop 1 and 2 for all ten stress-energy data sets, Tables 6 and 7.

Table 4: A and B Statistics Drop 1

Material (lb/ft^3)	A	B	Std. Error A	Std. Error B	Upper 95% CL A	Lower 95% CL A	Upper 95% CL B	Lower 95% CL B
S 1.90	30.71	0.052	6.65	0.006	46.41	18.46	0.065	0.041
T 1.90	18.66	0.043	2.33	0.004	24.26	13.86	0.051	0.035
U 1.30	11.45	0.068	2.05	0.005	16.50	7.48	0.080	0.057
U 1.50	13.65	0.056	2.30	0.004	19.29	9.10	0.067	0.047
U 1.90	21.43	0.039	2.30	0.003	26.80	16.78	0.046	0.033
X 1.00	16.33	0.071	1.76	0.003	20.24	12.96	0.079	0.065
X 1.25	17.31	0.065	1.26	0.002	20.07	14.84	0.070	0.061
X 1.50	20.35	0.053	2.11	0.003	25.00	16.33	0.059	0.047
X 1.75	18.83	0.051	1.44	0.002	22.08	15.90	0.056	0.047
X 2.20	29.16	0.032	2.32	0.002	34.45	24.48	0.037	0.028

Table 5: A and B Statistics Drop 2

Material (lb/ft3)	A	B	Std. Error A	Std. Error B	Upper 95% CL A	Lower 95% CL A	Upper 95% CL B	Lower 95% CL B
S 1.90	34.75	0.057	7.05	0.005	51.21	21.67	0.069	0.047
T 1.90	13.22	0.068	1.62	0.003	17.06	9.89	0.076	0.061
U 1.30	18.14	0.075	2.11	0.003	22.97	13.96	0.082	0.069
U 1.50	16.39	0.074	2.96	0.005	23.51	10.70	0.085	0.065
U 1.90	20.66	0.065	1.98	0.003	25.15	16.67	0.071	0.060
X 1.00	24.58	0.075	2.98	0.004	31.29	18.92	0.083	0.067
X 1.25	23.16	0.075	1.58	0.002	26.64	20.03	0.079	0.071
X 1.50	29.46	0.063	2.53	0.002	34.91	24.62	0.067	0.058
X 1.75	24.52	0.065	1.80	0.002	28.46	20.95	0.069	0.061
X 2.20	25.78	0.056	1.79	0.002	29.70	22.24	0.060	0.053

Table 6: Regression Analysis Drop 1 Stress-Energy Data

Material (lb/ft^3)	SSE $(lb/in^2)^2$	RMSE (lb/in^2)	r^2
S 1.90	10930.56	29.00	0.96
T 1.90	821.83	7.95	0.97
U 1.30	1512.31	10.79	0.98
U 1.50	1513.17	10.79	0.97
U 1.90	705.56	7.37	0.97
X 1.00	1764.95	9.90	0.99
X 1.25	921.39	7.15	0.99
X 1.50	2187.43	11.02	0.98
X 1.75	772.99	6.55	0.99
X 2.20	803.07	6.68	0.97

Table 7: Regression Analysis Drop 2 Stress-Energy Data

Material (lb/ft^3)	SSE $(lb/in^2)^2$	RMSE (lb/in^2)	r^2
S 1.90	15028.66	34.00	0.97
T 1.90	1135.66	9.35	0.99
U 1.30	2529.05	13.95	0.99
U 1.50	5576.20	20.71	0.99
U 1.90	1603.51	11.11	0.99
X 1.00	5802.95	17.96	0.99
X 1.25	2356.78	11.44	0.99
X 1.50	5142.35	16.90	0.99
X 1.75	2315.23	11.34	0.99
X 2.20	1876.72	10.21	0.99

Observing Tables 6 and 7, the r^2 values of all ten materials are above 0.96 and above 0.97 for the first and second drop, respectively. Such high coefficient of determination values would lead one to believe that the calculated stress-energy equations fit each data set very well. However, the r^2 value is sensitive to outliers and should be used with caution. In order to perform a more concise regression analysis, the root mean square error should be calculated in addition to the r^2 value. Low root mean square errors mean that the stress-energy equations represent their respective data sets very well with regards to the individual data points. For example, Material X 1.75 lb/ft^3 had an RMSE of 6.55 lb/in^2, which means on average, the actual Dynamic Stress data missed the stress-energy regression line by 6.55 lb/in^2. This value gives more information with regards to how close the actual Dynamic Stress was to the regression line.

It is important to note that even though Material S, density 1.90 lb/ft^3, had an r^2 value of 0.96 for drop 1, which is a considerably high value, the high root mean square error was 29.00 lb/in^2. The other nine data sets had root mean square errors all below 11.02 lb/in^2. For Drop 2, Material S 1.90 lb/ft^3 had an r^2 of 0.97, but a considerably high RMSE of 34.00 lb/in^2. The other nine data sets had root mean square errors all below 20.71 lb/in^2. These high RMSE values mean there might be a calculation error in the original data, the material could have had inconsistent properties, and additional testing may be necessary. By only evaluating the r^2 value, these errors may have gone unnoticed if were not for the additional RMSE analysis. Therefore, it is important to include the root mean square error analysis in addition to the r^2 value in order to detect for any large errors.

Phase II. In order to determine how the variation in the A and B constants effect a predicted cushion curve, the data from Tables 4 and 5 were used to create upper and lower confidence bounds for a range of drop heights and thicknesses. Using the upper and lower stress-energy equations determined for each density of Material X, upper and lower cushion curve bounds were generated using six combinations: thickness of 1 and 2 inches, and drop heights of 18 inch, 24 inch, and 36 inch. The six combinations for Material X 1.00 lb/ft^3 can be seen in Figure 12. The remaining density cushion curve bounds can be seen in Appendix C.

Comparing these six combinations, the variation between the upper and lower cushion curve bounds increases as drop height increases from 18 to 36 inches for all five densities. As thickness increases from 1 to 2 inches, the variation decreases between the upper and lower cushion curves for all five densities, particularly near the optimal static load. This would imply that the calculated stress-energy equation will most likely generate a cushion curve that will vary the least at lower drop heights when thickness remains constant, or at larger thicknesses when drop height remains constant. However, it should be noted that using the stress-energy method for predicting cushion curves, a drop height of 18 inches and a thickness of 1 inch will produce the same cushion curve as a drop height of 36 inches and a thickness of 2 inches because of the nature of Equation 5. Therefore, the variation seen between these two sets of cushion curves would be the same.

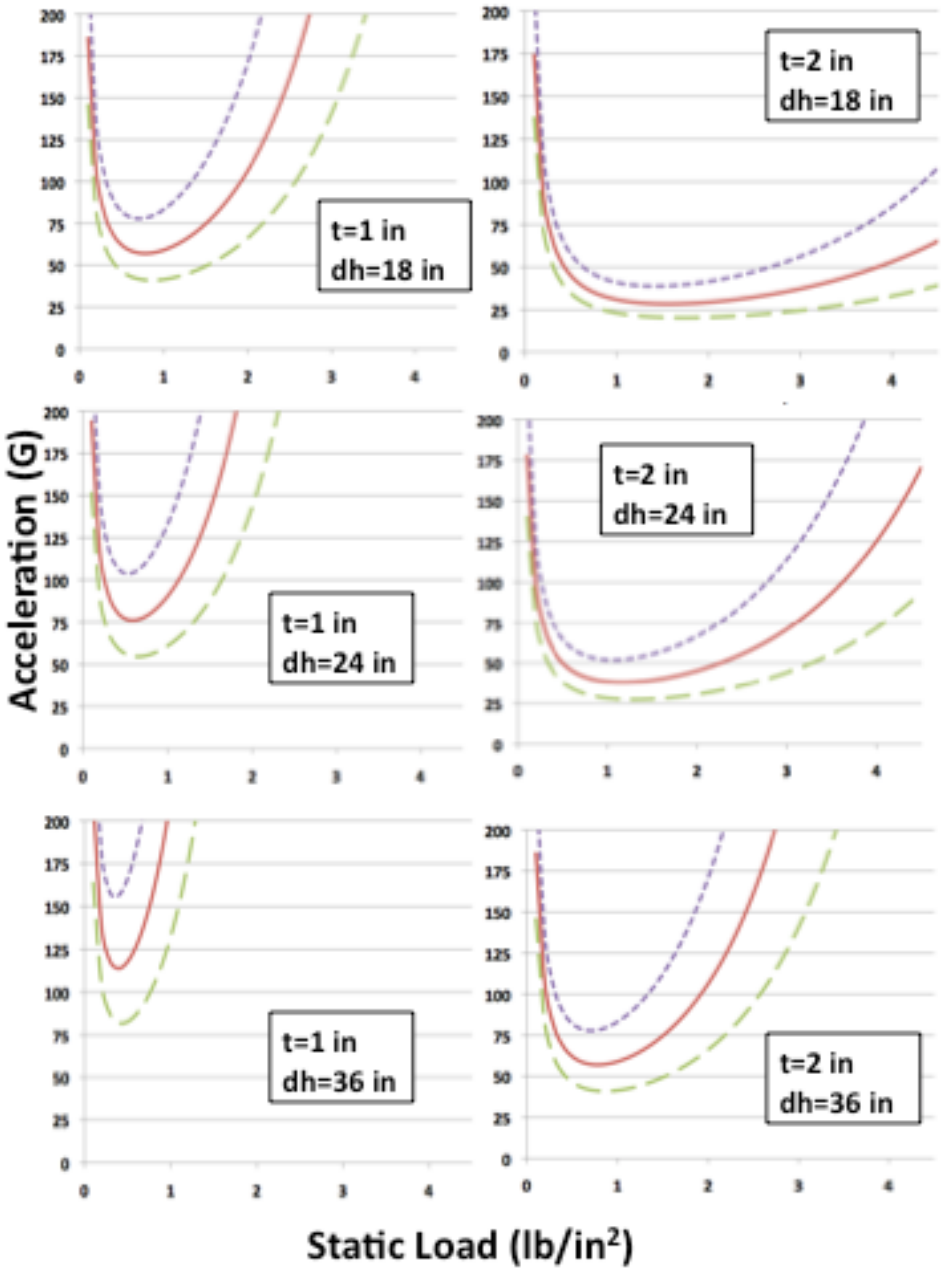

Figure 12: Upper and Lower Predicted Drop 1 Cushion Curve Bounds Material X 1.00 lb/ft^3

Phase III. Cushion curve data using the traditional ASTM D1596 method were tested at the various combinations of drop height and thicknesses seen in Table 3. Each actual cushion curve was then overlaid onto the corresponding upper and lower cushion curve bounds for the respective drop height and thickness combinations. The predicted cushion curve using the stress-energy method, the upper and lower cushion curve confidence bounds, and the actual ASTM D1596 cushion curve for Data Set C Drop 1 and Drop 2 can be seen in Figures 13 and 14. The remaining cushion curve data sets can be found in Appendix D.

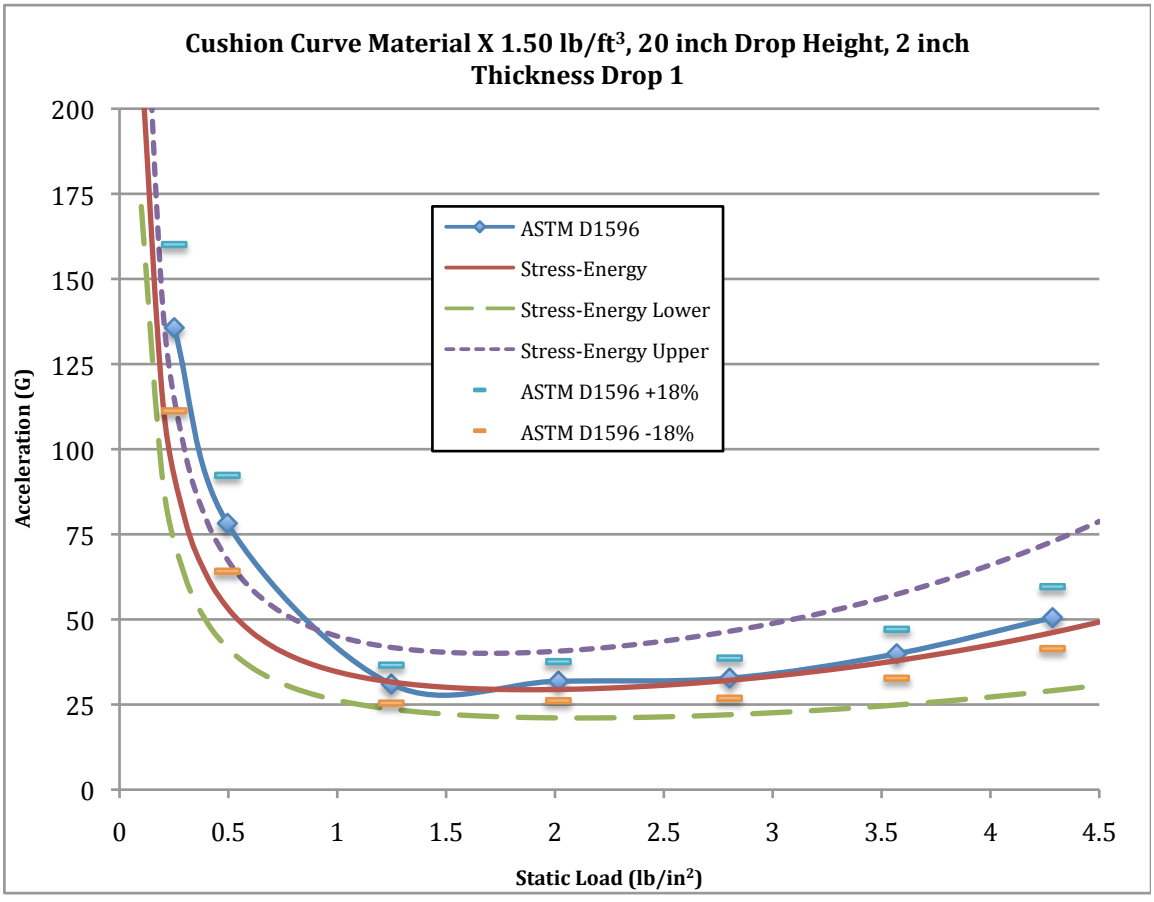

Figure 13: Cushion Curve Material X 1.50 lb/ft^3 20 inch Drop Height, 2 inch Thickness, Drop 1

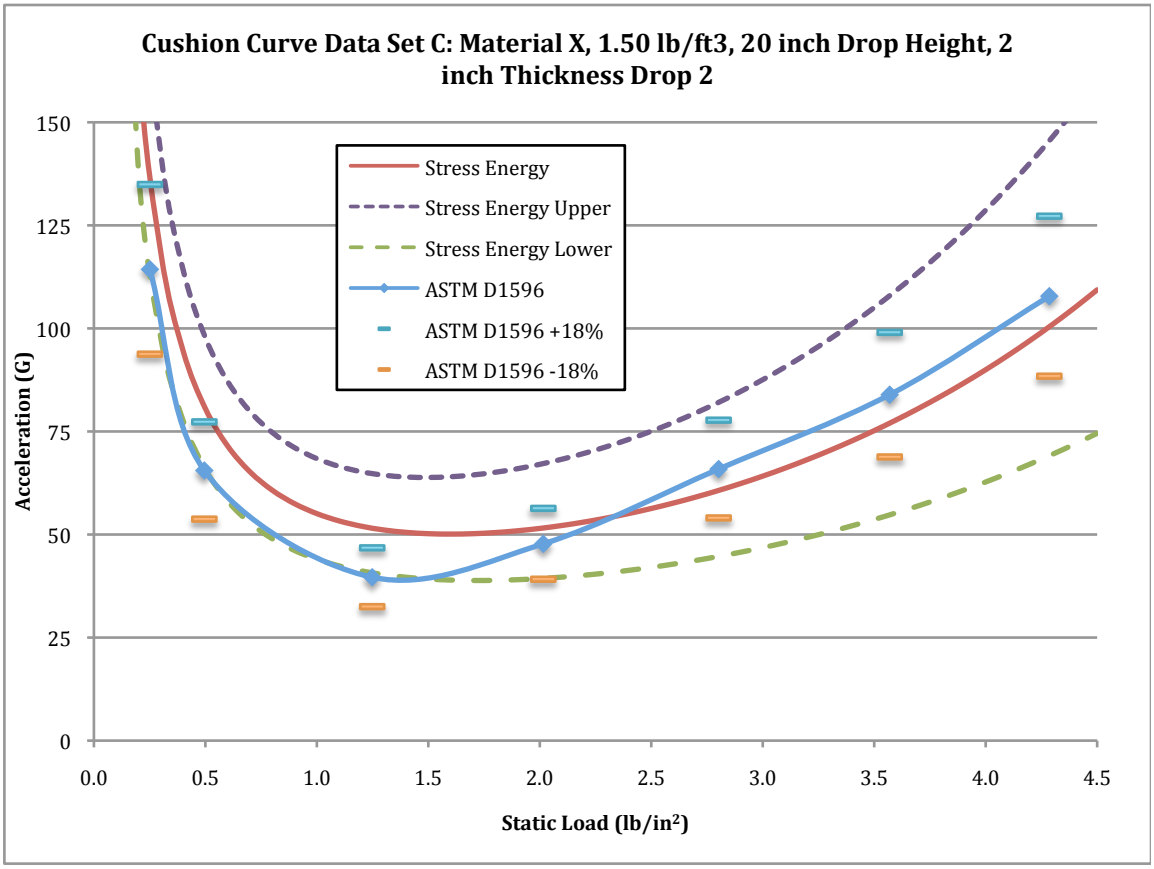

Figure 14: Cushion Curve Data Set C: Material X 1.50 lb/ft^3 20 inch Drop Height, 2 inch Thickness, Drop 2

For drop 1, the actual cushion curves appear to be close to the predicted cushion curves for 1.00 lb/ft^3, 1.25 lb/ft^3 and 1.50 lb/ft^3. The two 1.75 lb/ft^3 sets have actual cushion curves that are above the predicted accelerations for low static loads, and then begin to align more accurately as static load increases. The 2.20 lb/ft^3 data set show a trend similar to the 1.75 lb/ft^3 sets, but do not align as well as static load increases. All six data sets have maximum accuracy near the optimum static load, or just after the optimum static load. The greatest variation can be seen in very low static loads, as well as very high static loads, which correlates to the limitations of the cushioning ability of the foam at these regions. This same trend can be seen in all six drop 2 data sets as well. For

densities 1.00 lb/ft^3, 1.25 lb/ft^3 and 1.50 lb/ft^3, the actual cushion curve falls below the predicted cushion curve for low static loads. For both densities of 1.75 lb/ft^3 and 2.20 lb/ft^3, the actual cushion curve falls above the predicted cushion curve at low static loads.

At each static load tested using ASTM D1596, the absolute difference and absolute percent difference were calculated for drop 1 and 2 for Data Set C, Tables 8 and 9. The remaining cushion curve data set calculations can be seen in Appendix E. Because packaging engineers are focused on the optimum static load region, the average percent difference seen in Tables 8 and 9 are broken up into two sections: the average percent difference for the low static loads that would not be typically chosen for energy absorbing applications, and the average percent difference for the remaining recommended static loads. The high percent difference for the low static loads may not be considered problematic since these static loads are not usually chosen for energy absorption applications.

Table 8: Difference and Percent Difference Material X, 1.50 lb/ft^3 Drop 1

Static Load (lb/in^2)	Stress-Energy Predicted Acceleration (G's)	ASTM D1596 Acceleration (G's)	Difference (G's)	Percent Difference (%)	Average Percent Difference (%)
0.25	93.0	135.7	42.7	31.5	32.5
0.50	52.1	78.2	26.2	33.4	
1.25	31.6	31.0	0.6	2.0	
2.02	29.4	31.9	2.4	7.6	
2.80	32.1	32.8	0.6	2.0	5.0
3.57	37.9	39.9	2.0	5.1	
4.29	46.2	50.5	4.3	8.5	

Table 9: Difference and Percent Difference Material X, 1.50 lb/ft^3 Drop 2

Static Load (lb/in^2)	Stress-Energy Predicted Acceleration (G's)	ASTM D1596 Acceleration (G's)	Difference (G's)	Percent Difference (%)	Average Percent Difference (%)
0.25	137.8	114.3	23.4	20.5	21.7
0.50	80.6	65.5	15.0	22.9	
1.25	51.5	39.6	11.9	30.0	11.5
2.02	51.6	47.8	3.9	8.1	
2.80	60.7	65.9	5.2	7.9	
3.57	79.8	83.9	4.2	5.0	
4.29	100.6	107.8	7.2	6.7	

For drop 1, the lowest percent difference for recommended static loads was 5.03%, Data Set C, and the highest percent difference was 22.39%, Data Set E, with an average of 11.95%. For drop 2, the lowest and highest percent difference was 8.51%, Data Set F, and 19.35%, Data Set E, with an average of 13.24%. The greatest percent differences for both drops for all six data sets typically occurred at the lowest and highest static loads, with minimum errors at the middle static loads.

The maximum 18% between lab error allowed by ASTM D1596, represented as the bars on Figures 13 and 14, were calculated for Drop 1 and 2, Tables 10 and 11. The error calculations for the remaining data sets can be seen in Appendix F. The accelerations listed in the 18% error columns represent the maximum and minimum accelerations allowed by the 18% error that could be seen between labs at the same drop height and thickness. The last column lists whether or not the predicted acceleration value found by using the stress-energy equation fell within the 18% error at each static load. A yes indicates that the predicted acceleration using the stress-energy method falls within the 18% error allowed by ASTM D1596 for between labs. No indicates that the predicted acceleration using the stress-energy method did not fall within the 18% error. If it did not

fall within the error limit, the number of G's the predicted stress energy acceleration missed the nearest limit is also listed. It may be of interest to do this same comparison method using the three sigma calculations of the standard deviation of the ASTM D1596 accelerations.

Table 10: Error Allowed by ASTM D1596 for Material X, 1.50 lb/ft^3 Drop 1

Static Load (lb/in^2)	Stress-Energy Predicted Acceleration (G's)	ASTM D1596 Acceleration (G's)	+18% Error (G's)	-18% Error (G's)	Did Predicted Fall Within Error?	Missed Closest Limit By (G's)
0.25	93.0	135.7	160.1	111.3	No	18.29
0.50	52.1	78.2	92.3	64.2	No	12.08
1.25	31.6	31.0	36.6	25.4	Yes	-
2.02	29.4	31.9	37.6	26.1	Yes	-
2.80	32.1	32.8	38.6	26.9	Yes	-
3.57	37.9	39.9	47.1	32.7	Yes	-
4.29	46.2	50.5	59.6	41.4	Yes	-

Table 11: Error Allowed by ASTM D1596 for Material X, 1.50 lb/ft^3 Drop 1

Static Load (lb/in^2)	Stress-Energy Predicted Acceleration (G's)	ASTM D1596 Acceleration (G's)	+18% Error (G's)	-18% Error (G's)	Did Predicted Fall Within Error?	Missed Closest Limit By (G's)
0.25	137.8	114.3	134.9	93.8	No	2.27
0.50	80.6	65.5	77.3	53.7	No	3.75
1.25	51.5	39.6	46.8	32.5	No	4.76
2.02	51.6	47.8	56.3	39.2	Yes	-
2.80	60.7	65.9	77.7	54.0	Yes	-
3.57	79.8	83.9	99.0	68.8	Yes	-
4.29	100.6	107.8	127.2	88.4	Yes	-

Two data sets produced ASTM D1596 cushion curves that did not correlate as well with the predicted cushion curves, particularly for low and optimum static loads: drop 1 for Material X 1.75 lb/ft^3, 18 inch drop height, one inch thickness, seen in Figure 15, and Material X 1.75 lb/ft^3 36 inch drop height, two inch thickness, found in Appendix D. Both of these data sets produced ASTM D1596 cushion curves with much higher

accelerations than the predicted cushion curves for static loads below 1.5 lb/in^2. This can possibly be explained by two factors. The first is that these two data sets represent the extremes of the drop height choices. At a drop height of 36 inches, there might be variation in the recorded accelerations due to the high drop height. At a drop height of 18 inches, at these low static loads, the foam may not have been able to deflect due to a low weight. The other explanation may be that during the stress-energy testing, no static load was tested below 0.86 lb/in^2. There is a possibility that the stress-energy method may not be as successful in predicting the performance of foam at static loads that are not utilized in the original stress-energy testing. Both drop 2 comparisons displayed much closer acceleration values

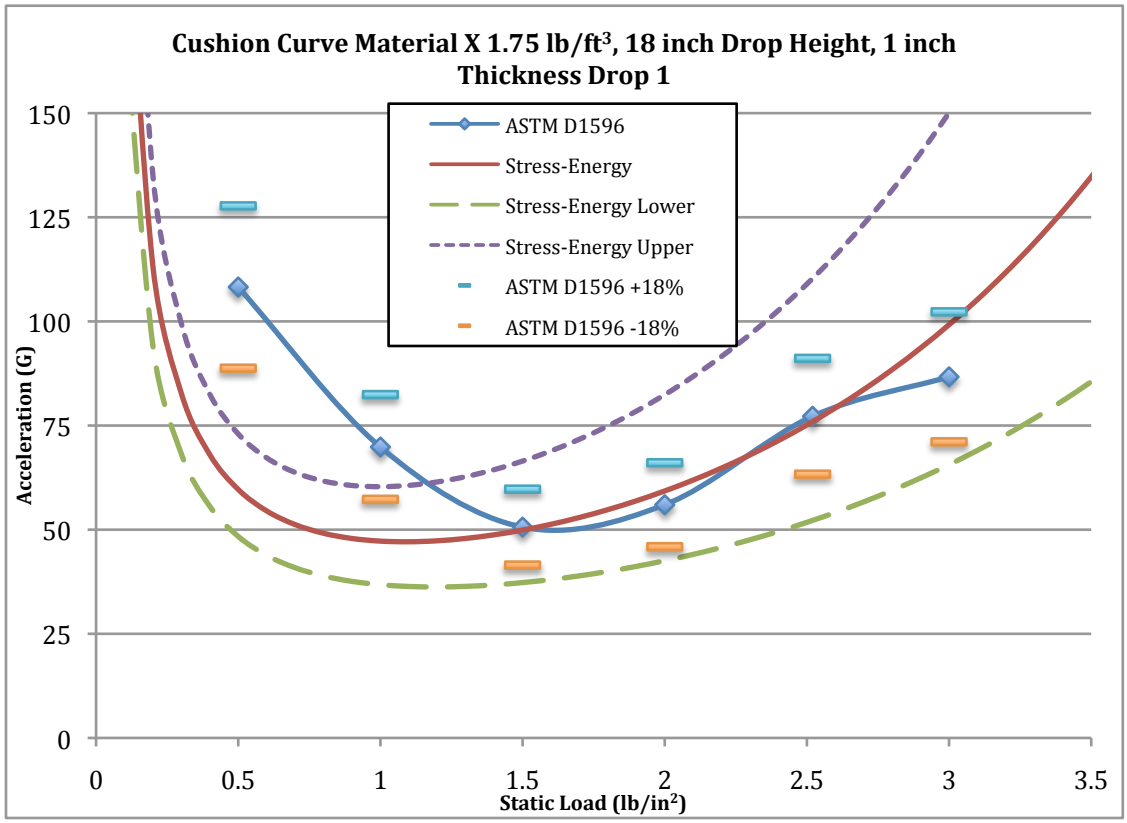

Figure 15: Cushion Curve Data Set D: Material X 1.75 lb/ft^3 18 inch Drop Height, 1 inch Thickness, Drop 1

For the 34 total recommended static loads, 27 fell within the 18% error for Drop 1, and 25 fell within the error for Drop 2. Again, the static loads near the optimum static load were more likely to fall within the error than the low and high static loads. For the remaining recommended static loads that did not fall within the error, the average missed acceleration to the nearest limit was 13.3 G's for drop 1 and 17.4 G's for drop 2.

It should be noted that it took about an average of 6 hours to complete a traditional cushion curve using ASTM D1596, which displays the accelerations for one drop height and one thickness. It took about an average of 10 hours to complete the stress-energy method for one material, which includes testing for the maximum and minimum energy levels, that could then be used to create a cushion curve for any reasonable drop height and thickness. Both time assessments include cushion prep, cushion testing, and data analysis.

CHAPTER FIVE

CONCLUSIONS:

In order to determine how well the stress-energy method can predict cushion curves, ten stress-energy data sets were analyzed using regression analysis in addition to calculating the coefficient of determination. Confidence bounds were determined for various predicted cushion curves for five of these materials at various drop height and thickness combinations. These combinations were then tested using ASTM D1596 in order to compare how close actual accelerations were to predicted cushion curves.

By analyzing ten data sets that utilize the stress-energy method to describe the cushioning properties of drops 1 and 2, it was found that every respective stress-energy equation produced an r^2 value greater than 0.96 for Drop 1 and 0.97 for Drop 2. However, the r^2 value alone is not sufficient enough to explain the goodness of fit of the stress-energy equation. The root mean square error is a measure of the average miss of the predicted stress to the actual stress and should be calculated in addition to the r^2 value. The root mean square error for drop 1 ranged from 6.6 lb/in^2 to 11.0 lb/in^2, with the exception of Material S, density 1.50 lb/in^2, which had an RMSE of 29.0 lb/in^2. For drop 2, the RMSE ranged from 9.4 lb/in^2 to 20.7 lb/in^2, with the exception of Material S, density 1.90lb/ft^3, which had an RMSE of 34.0 lb/in^2. When a high RMSE value occurs, such as with Material S, one can suspect that there was error in the data collection or material variation and additional testing may be necessary even though the coefficient of determination value was very high. The RMSE should be calculated in addition to the coefficient of determination in order to detect for discrepancies such as these. Because of

the low RMSE values and high coefficient of determination values, each stress-energy equation accurately reflected the data collected for each data set.

Upper and lower cushion curve confidence bounds created using the upper and lower 95% confidence levels for the A and B constants can show the variation that might be seen between laboratory testing. The calculated stress-energy equation will most likely generate a cushion curve that will vary the least at lower drop heights when thickness remains constant, or at larger thicknesses when drop height remains constant. This may be beneficial in order to make predications or comparisons with regards to what variation might occur, particularly when looking at extreme drop heights or thicknesses.

By comparing six sets of actual Drop 1 and 2 cushion curves created using ASTM D1596 to those predicted using the stress-energy method, many positive results can be seen. All six data sets have maximum accuracy near the optimum static load, or just after the optimum static load. The greatest variation can be seen in very low static loads, as well as very high static loads, which correlates to the limitations of the cushioning ability of the foam at these regions.

For drop 1, the lowest average percent difference for recommended static loads between actual and predicted accelerations for the six data sets was 5.03% and the highest percent difference was 22.39%, with an average of 11.95%. For drop 2, the lowest and highest percent difference was 8.51% and 19.35%, with an average of 13.24%. The greatest percent differences for both drops for all six data sets typically occurred at the lowest and highest static loads, with minimum errors at the middle static loads. Packaging designers often choose to use static loads that produce the lowest acceleration values. Very low static loads are used for blocking and bracing and are not

typically used for energy absorption applications. Because of this, high percent differences seen for low static loads may not be considered problematic.

It may be beneficial to conduct stress-energy testing using combinations of drop height, static load, and cushion thickness that correlate to the expected characteristics of the desired material. The greatest variation occurred in data sets with extremely low static loads that were not tested using the stress-energy method. The stress-energy method may not be as accurate in predicting the performance at low static loads that are not utilized during stress-energy testing.

For the 34 total recommended static loads, 27 fell within the 18% between laboratory error stated by ASTM D1596 for Drop 1, and 25 fell within the error for Drop 2. Again, the static loads near the optimum static load were more likely to fall within the error than the low and high static loads. For the remaining recommended static loads that did not fall within the error, the average missed acceleration to the nearest limit was 13.3 G's for drop 1 and 17.4 G's for drop 2.

In general, the data from this study suggests that the stress-energy generated cushion curves yield acceleration values that are similar to the actual acceleration values for the static loads that would be typically chosen for energy absorption applications. The root mean square error, when used in addition to the r^2 value, may provide additional information as to the goodness of fit of the respective stress-energy equation. Confidence bounds using the upper and lower confidence levels of the A and B constants show the variation expected between labs. When actual ASTM D1596 cushion curves were compared to predicted cushion curves using the stress-energy method for five materials, positive results were seen. The majority of recommended static loads fell within the

between lab error allowed by ASTM D1596, and there were low average percent errors. In addition to producing cushion curves for exact drop heights and thicknesses, the reduction of testing time and material are also benefits from using the stress-energy method.

APPENDICES

Appendix A:

Test specifications for the stress-energy method for Material X.

Table 1: Testing Specifications for Material X 1.00 lb/ft^3

Sample	Expected Energy	Area (in^2)	Weight (lbs)	Static Load (lb/in^2)	Drop Height (in)	Thickness (in)
1.0_1.1	15	16.00	13.73	0.86	17.50	1.00
1.0_1.2	15	16.00	20.00	1.25	12.00	1.00
1.0_1.3	15	16.00	20.00	1.25	18.00	1.50
1.0_1.4	15	16.00	32.66	2.04	14.70	2.00
1.0_E4	15	16.00	45.68	2.86	10.50	2.00
1.0_2.1	22	16.00	20.00	1.25	17.60	1.00
1.0_2.2	22	16.00	32.66	2.04	10.80	1.00
1.0_2.3	22	16.00	32.66	2.04	16.20	1.50
1.0_E3	22	16.00	45.68	2.86	11.60	1.50
1.0_2.5	22	16.00	32.66	2.04	21.50	2.00
1.0_3.1	29	16.00	32.66	2.04	14.20	1.00
1.0_3.2	29	16.00	45.68	2.86	15.70	1.50
1.0_3.3	29	16.00	32.66	2.04	21.30	1.50
1.0_3.4	29	16.00	45.68	2.86	20.20	2.00
1.0_3.5	29	16.00	32.66	2.04	28.50	2.00
1.0_E1	35	16.00	32.66	2.04	17.10	1.00
1.0_4.2	35	16.00	45.68	2.86	18.80	1.50
1.0_4.3	35	16.00	32.66	2.04	25.70	1.50
1.0_E5	35	16.00	45.68	2.86	24.50	2.00
1.0_4.5	35	16.00	51.95	3.25	21.50	2.00

Table 2: Testing Specifications for Material X 1.25 lb/ft^3

Sample	Expected Energy	Area (in^2)	Weight (lbs)	Static Load (lb/in^2)	Drop Height (in)	Thickness (in)
1.25_1.1	15	16.00	13.73	0.86	17.50	1.00
1.25_1.2	15	16.00	20.00	1.25	12.00	1.00
1.25_1.3	15	16.00	20.00	1.25	18.00	1.50
1.25_1.4	15	16.00	32.66	2.04	14.70	2.00
1.25_1.5	15	16.00	45.68	2.86	10.50	2.00
1.25_2.1	22	16.00	20.00	1.25	17.60	1.00
1.25_2.2	22	16.00	32.66	2.04	10.80	1.00
1.25_2.3	22	16.00	32.66	2.04	16.20	1.50
1.25_E3	22	16.00	45.68	2.86	11.60	1.50
1.25_2.5	22	16.00	32.66	2.04	21.50	2.00
1.25_3.1	29	16.00	32.66	2.04	14.20	1.00
1.25_3.2	29	16.00	32.66	2.04	21.30	1.50
1.25_3.3	29	16.00	45.68	2.86	15.20	1.50
1.25_E4	29	16.00	45.68	2.86	20.30	2.00
1.25_3.5	29	16.00	32.66	2.04	28.50	2.00
1.25_4.1	35	16.00	32.66	2.04	17.10	1.00
1.25_E6	35	16.00	45.68	2.86	18.40	1.50
1.25_4.3	35	16.00	32.66	2.04	25.70	1.50
1.25_4.4	35	16.00	51.95	3.25	21.60	2.00
1.25_E5	35	16.00	45.68	2.86	24.50	2.00

Table 3: Testing Specifications for Material X 1.50 lb/ft^3

Sample	Expected Energy	Area (in^2)	Weight (lbs)	Static Load (lb/in^2)	Drop Height (in)	Thickness (in)
1.5_1.1	15	16.00	13.73	0.86	17.50	1.00
1.5_1.2	15	16.00	20.00	1.25	12.00	1.00
1.5_1.3	15	16.00	20.00	1.25	18.00	1.50
1.5_E2	15	16.00	32.66	2.04	14.70	2.00
1.5_1.5	15	16.00	45.68	2.86	10.50	2.00
1.5_2.1	23	16.00	20.00	1.25	18.40	1.00
1.5_2.2	23	16.00	32.66	2.04	11.30	1.00
1.5_2.3	23	16.00	32.66	2.04	16.90	1.50
1.5_2.4	23	16.00	45.68	2.86	12.10	1.50
1.5_2.5	23	16.00	32.66	2.04	22.50	2.00
1.5_3.1	31	16.00	32.66	2.04	15.20	1.00
1.5_3.2	31	16.00	45.68	2.86	16.30	1.50
1.5_3.3	31	16.00	32.66	2.04	22.80	1.50
1.5_3.4	31	16.00	45.68	2.86	21.70	2.00
1.5_3.5	31	16.00	32.66	2.04	30.40	2.00
1.5_4.1	40	16.00	32.66	2.04	19.60	1.00
1.5_4.2	40	16.00	45.68	2.86	21.00	1.50
1.5_4.3	40	16.00	32.66	2.04	29.40	1.50
1.5_4.4	40	16.00	45.68	2.86	28.00	2.00
1.5_4.5	40	16.00	51.95	3.25	24.70	2.00

Table 4: Testing Specifications for Material X 1.75 lb/ft^3

Sample	Expected Energy	Area (in^2)	Weight (lbs)	Static Load (lb/in^2)	Drop Height (in)	Thickness (in)
1.75_1.1	15	16.00	13.73	0.86	17.50	1.00
1.75_1.2	15	16.00	20.00	1.25	12.00	1.00
1.75_E3	15	16.00	20.00	1.25	18.00	1.50
1.75_1.4	15	16.00	32.66	2.04	14.70	2.00
1.75_1.5	15	16.00	45.68	2.86	10.50	2.00
1.75_2.1	23	16.00	20.00	1.25	18.40	1.00
1.75_2.2	23	16.00	32.66	2.04	11.30	1.00
1.75_2.3	23	16.00	32.66	2.04	16.90	1.50
1.75_2.4	23	16.00	45.68	2.86	12.10	1.50
1.75_2.5	23	16.00	32.66	2.04	22.50	2.00
1.75_E1	31	16.00	32.66	2.04	15.20	1.00
1.75_3.2	31	16.00	45.68	2.86	16.20	1.50
1.75_3.3	31	16.00	32.66	2.04	22.80	1.50
1.75_3.4	31	16.00	45.68	2.86	21.70	2.00
1.75_3.5	31	16.00	32.66	2.04	30.40	2.00
1.75_4.1	40	16.00	32.66	2.04	19.60	1.00
1.75_4.2	40	16.00	45.68	2.86	21.00	1.50
1.75_4.3	40	16.00	51.95	3.25	18.50	1.50
1.75_4.4	40	16.00	51.95	3.25	24.70	2.00
1.75_4.5	40	16.00	45.88	2.87	27.90	2.00

Table 5: Testing Specifications for Material X 2.20 lb/ft^3

Sample	Expected Energy	Area (in^2)	Weight (lbs)	Static Load (lb/in^2)	Drop Height (in)	Thickness (in)
2.2_1.1	20	16.00	32.66	2.04	9.80	1.00
2.2_1.2	20	16.00	20.00	1.25	16.00	1.00
2.2_1.3	20	16.00	32.66	2.04	14.70	1.50
2.2_1.4	20	16.00	32.66	2.04	19.60	2.00
2.2_1.5	20	16.00	45.68	2.86	14.00	2.00
2.2_2.1	28	16.00	20.00	1.25	22.40	1.00
2.2_2.2	28	16.00	32.66	2.04	13.70	1.00
2.2_2.3	28	16.00	32.66	2.04	20.50	1.50
2.2_2.4	28	16.00	45.68	2.86	14.70	1.50
2.2_2.5	28	16.00	45.68	2.86	19.60	2.00
2.2_3.1	36	16.00	32.66	2.04	17.60	1.00
2.2_3.2	36	16.00	51.95	3.25	16.60	1.50
2.2_3.3	36	16.00	45.68	2.86	18.90	1.50
2.2_3.4	36	16.00	45.68	2.86	25.20	2.00
2.2_3.5	36	16.00	51.95	3.25	22.20	2.00
2.2_E1	45	16.00	32.66	2.04	22.00	1.00
2.2_4.2	45	16.00	51.95	3.25	20.80	1.50
2.2_4.3	45	16.00	45.68	2.86	23.60	1.50
2.2_4.4	45	16.00	45.68	2.86	31.50	2.00
2.2_4.5	45	16.00	51.95	3.25	27.70	2.00

APPENDIX B:

Stress-Energy data and fitted regression line for Material X. Values on the Dynamic Stress axis have been removed for proprietary reasons.

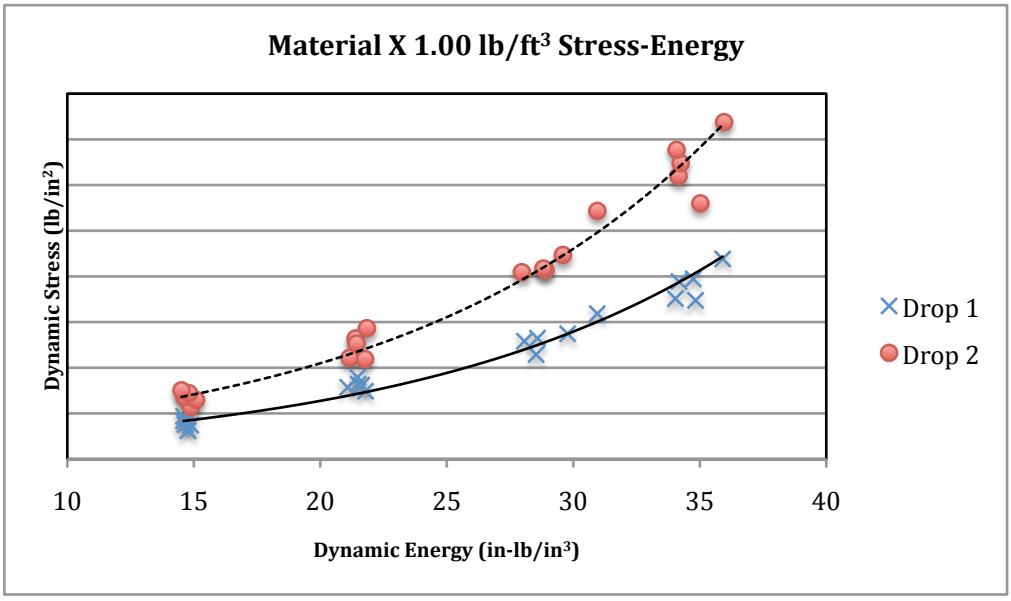

Figure 1: Stress-Energy Plot Material X 1.00 lb/ft^3

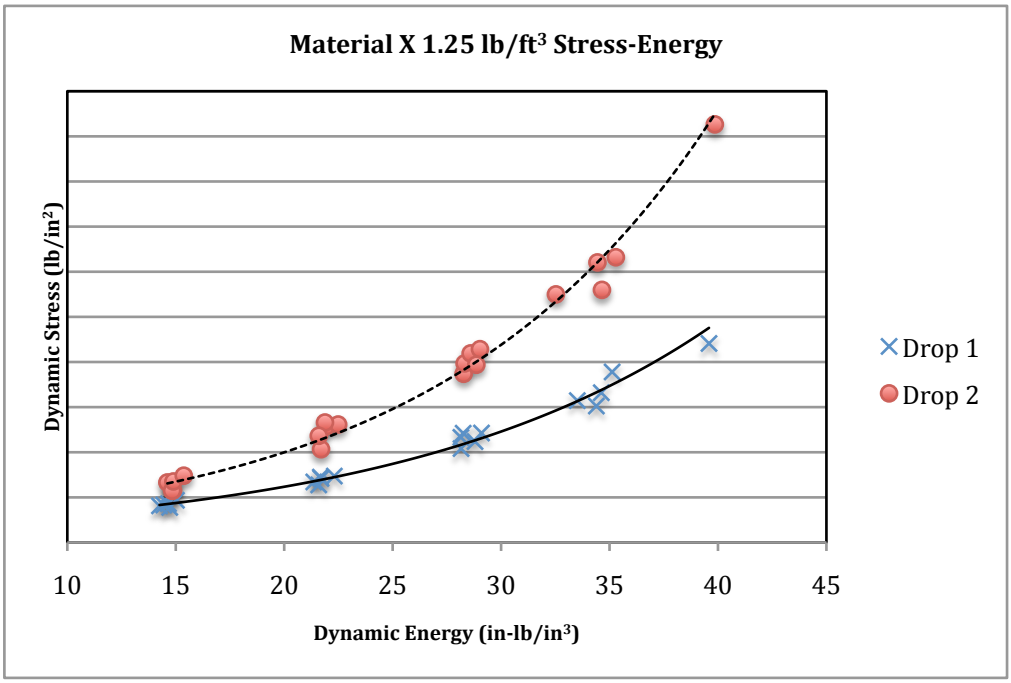

Figure 2: Stress-Energy Plot Material X 1.25 lb/ft^3

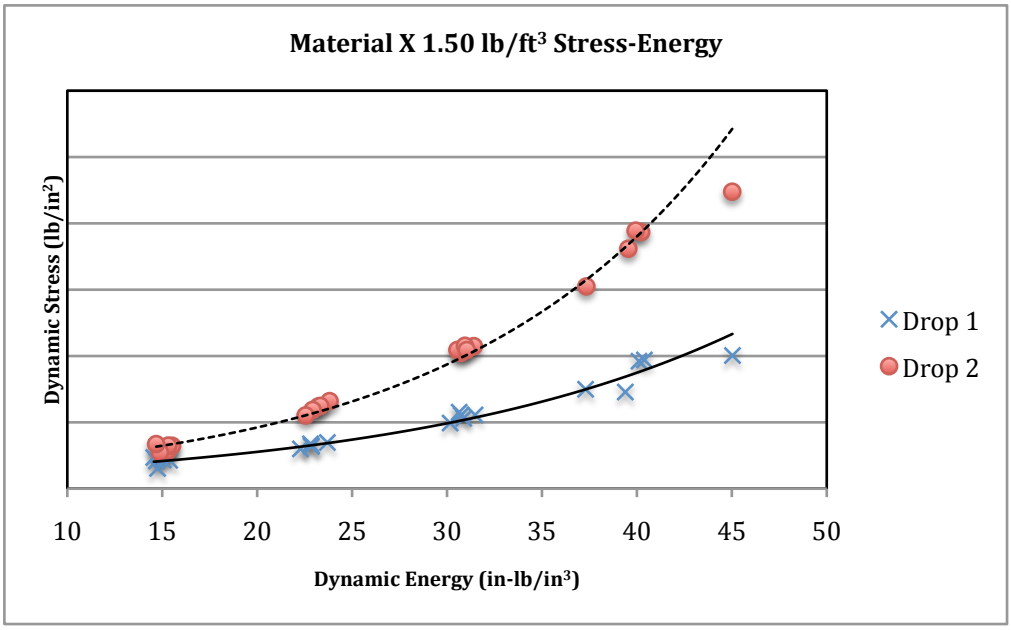

Figure 3: Stress-Energy Plot Material X 1.50 lb/ft^3

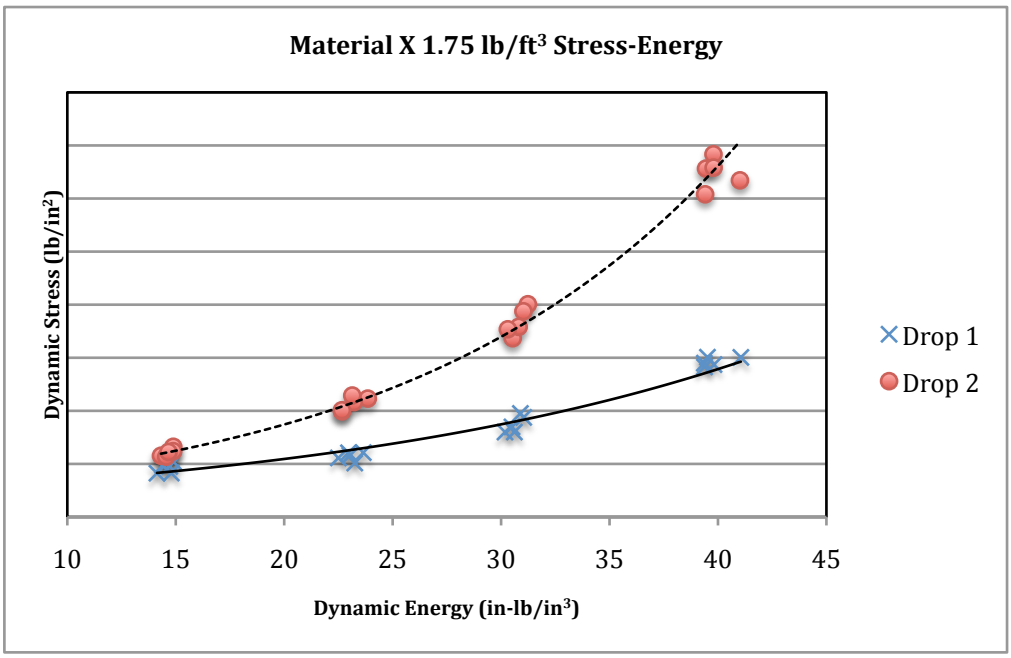

Figure 4: Stress-Energy Plot Material X 1.75 lb/ft^3

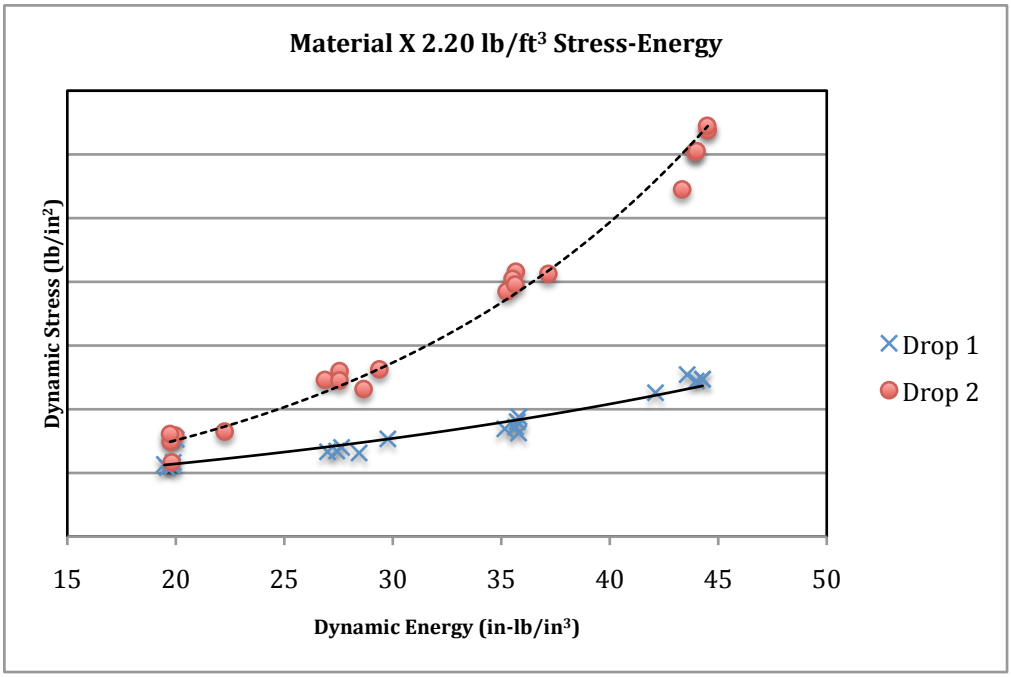

Figure 5: Stress-Energy Plot Material X 2.20 lb/ft^3

APPENDIX C:

Upper and lower cushion curve confidence bounds combinations drop 1. Cushion curves generated using the upper and lower stress-energy equations at six combinations of drop height and thickness: 1 and 2 inch thickness, 18 inch, 24 inch and 36 inch drop height.

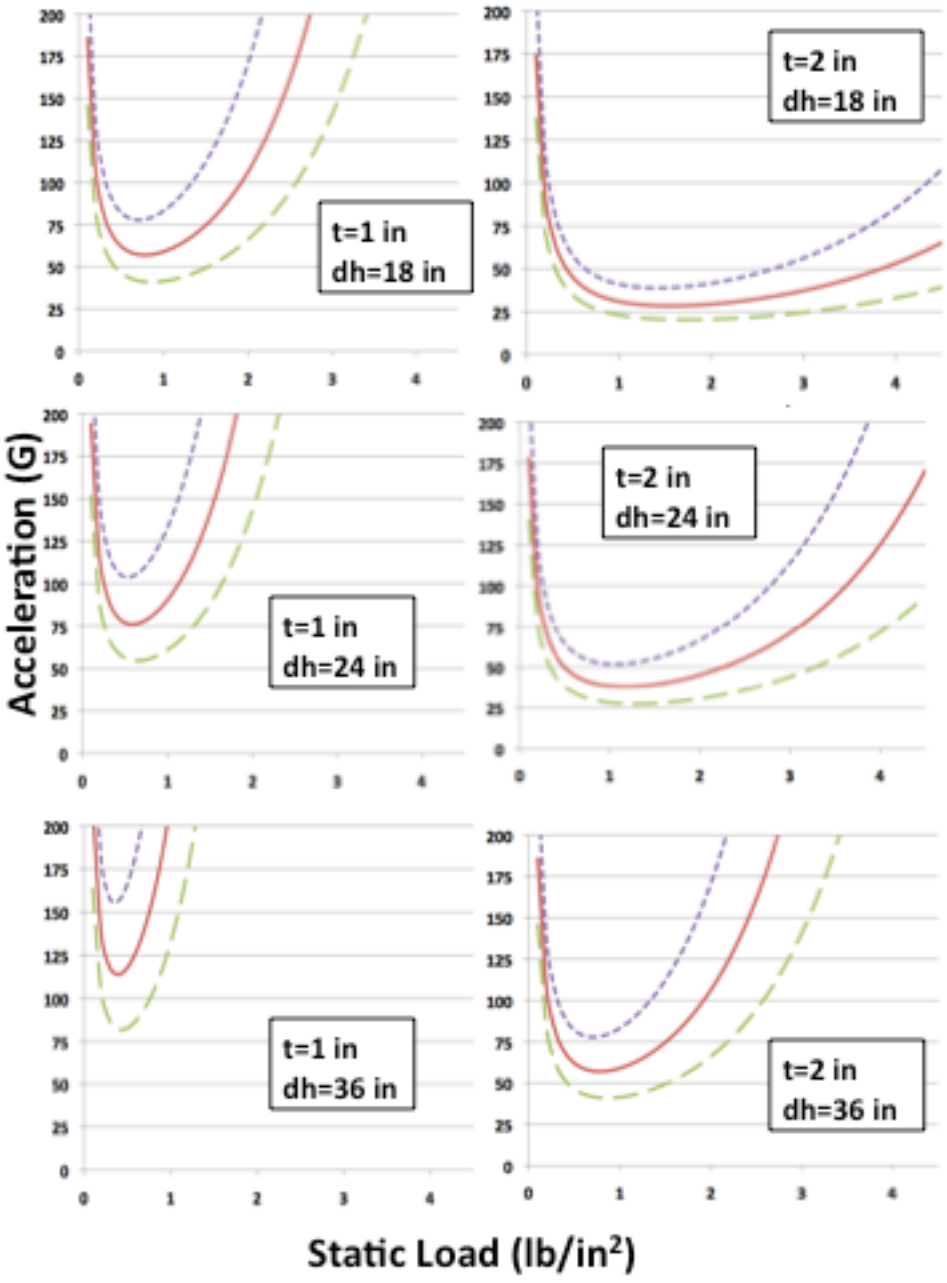

Figure 1: Material X 1.00 lb/ft^3 Predicted Drop 1 Cushion Curves

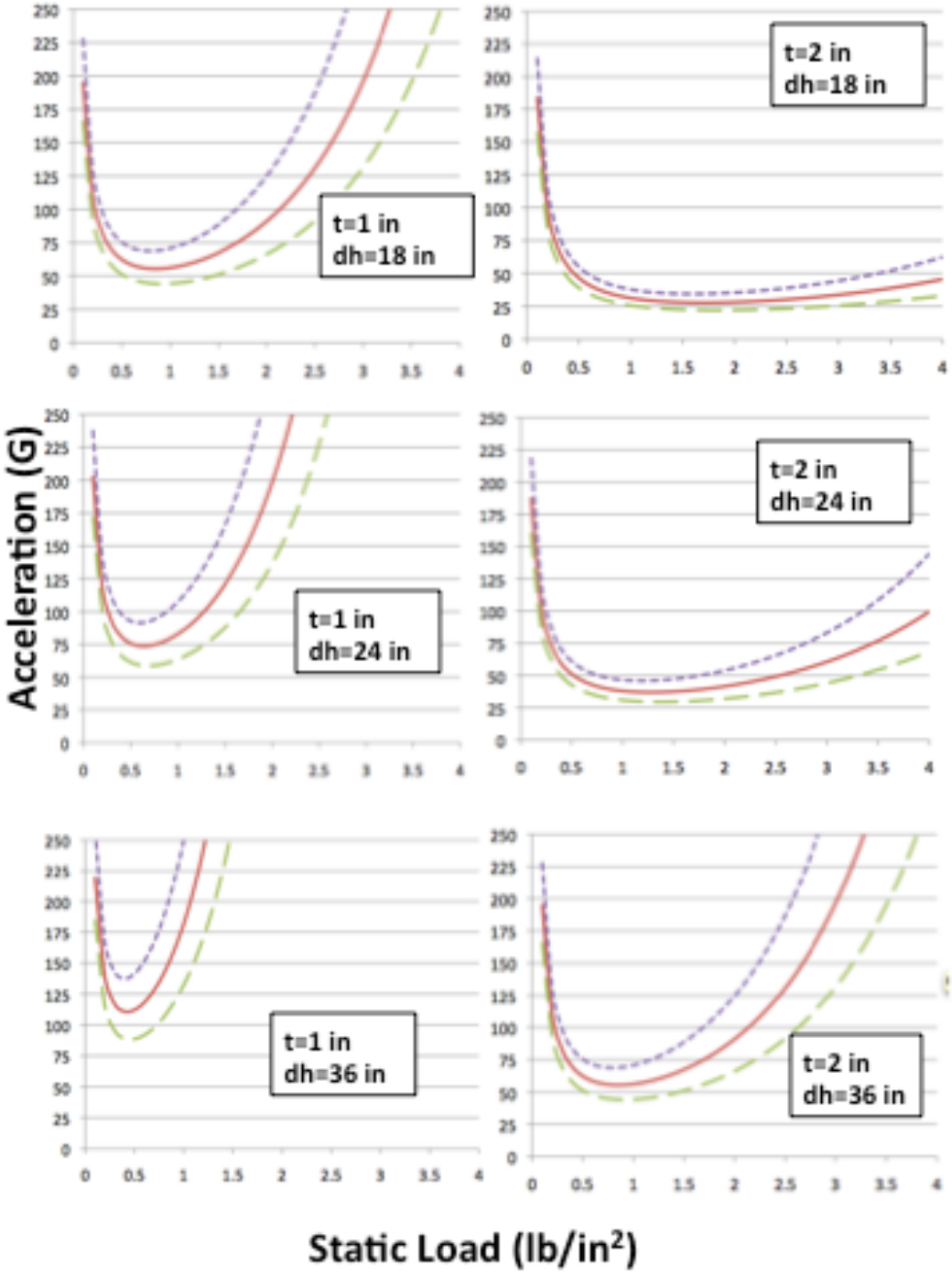

Figure 2: Material X 1.25 lb/ft^3 Predicted Drop 1 Cushion Curves

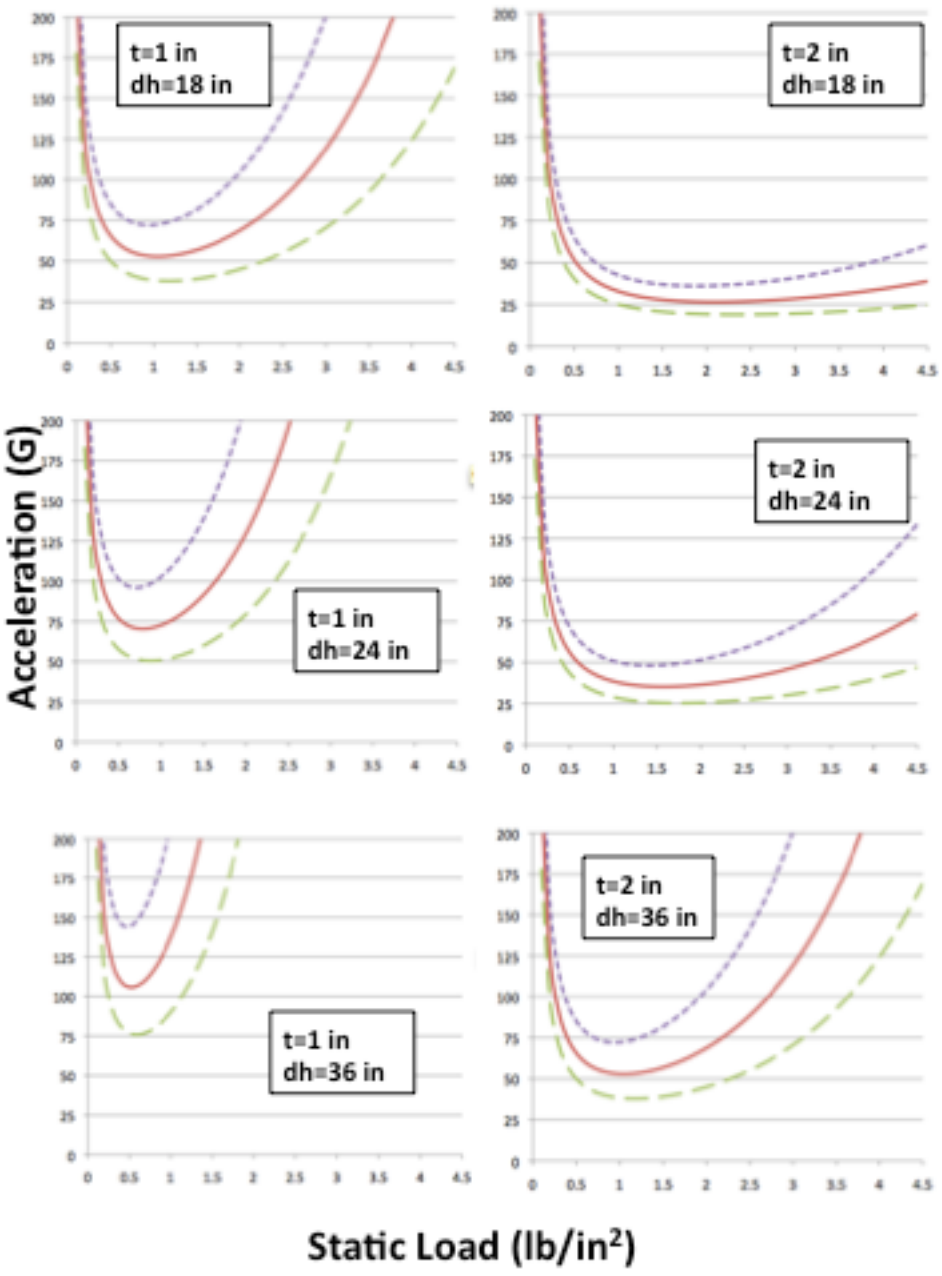

Figure 3: Material X 1.50 lb/ft^3 Predicted Drop 1 Cushion Curves

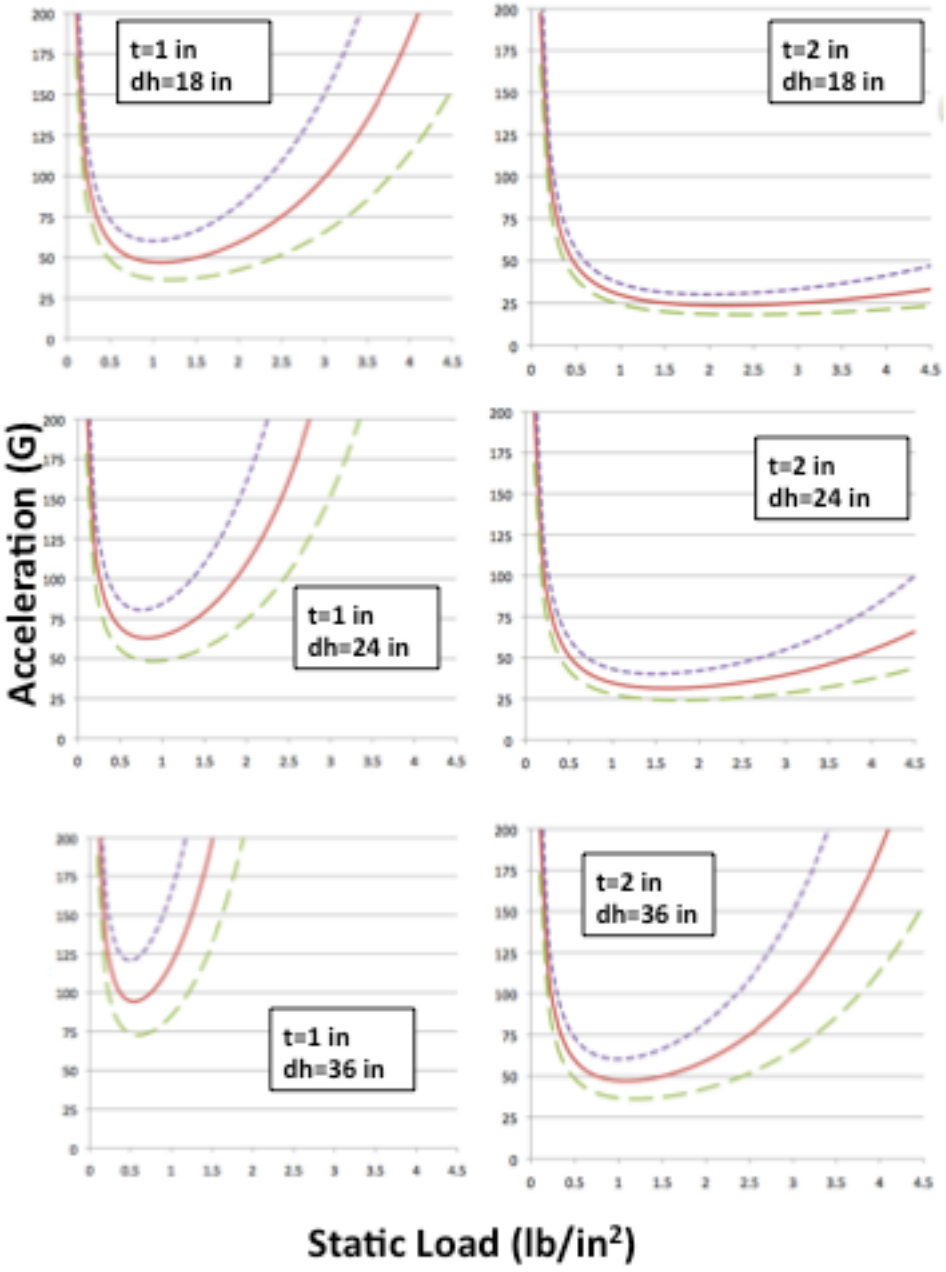

Figure 4: Material X 1.75 lb/ft^3 Predicted Drop 1 Cushion Curves

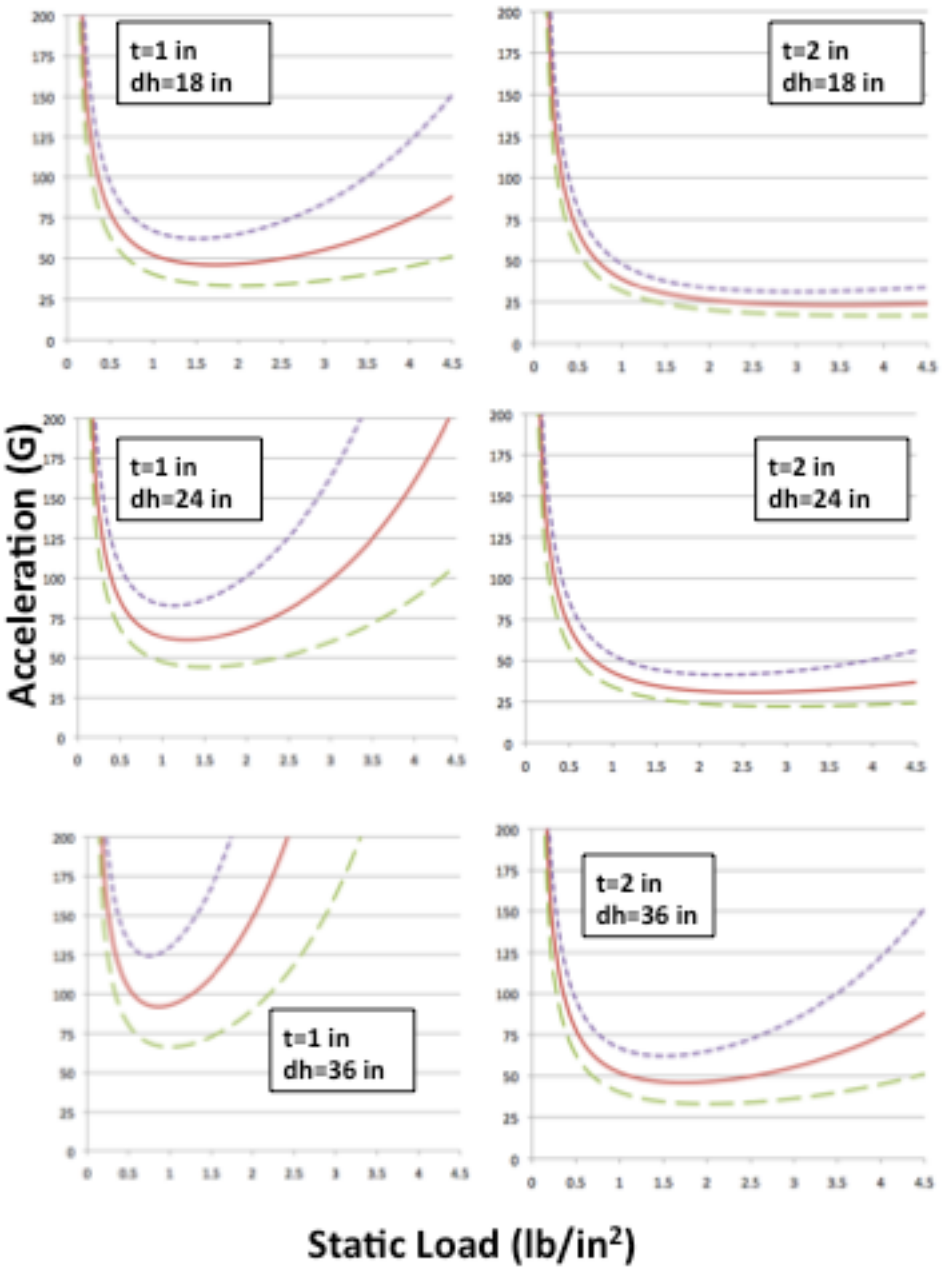

Figure 5: Material X 2.20 lb/ft^3 Predicted Drop 1 Cushion Curves

APPENDIX D:

Predicted cushion curves using the stress-energy method, upper and lower confidence bounds, actual ASTM D1596 cushion curve and ASTM 18% error ranges for Drops 1 and 2.

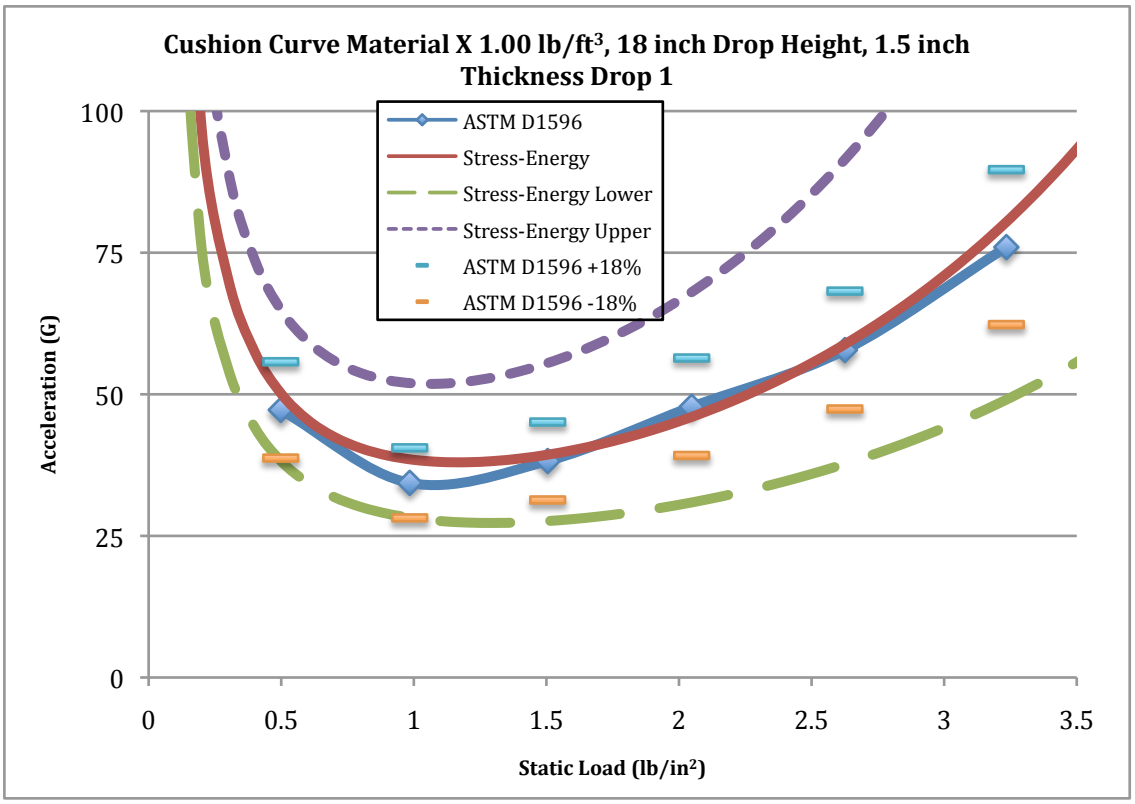

Figure 1: Predicted and Actual Cushion Curves, Confidence Bounds, ASTM Error Data Set A Drop 1

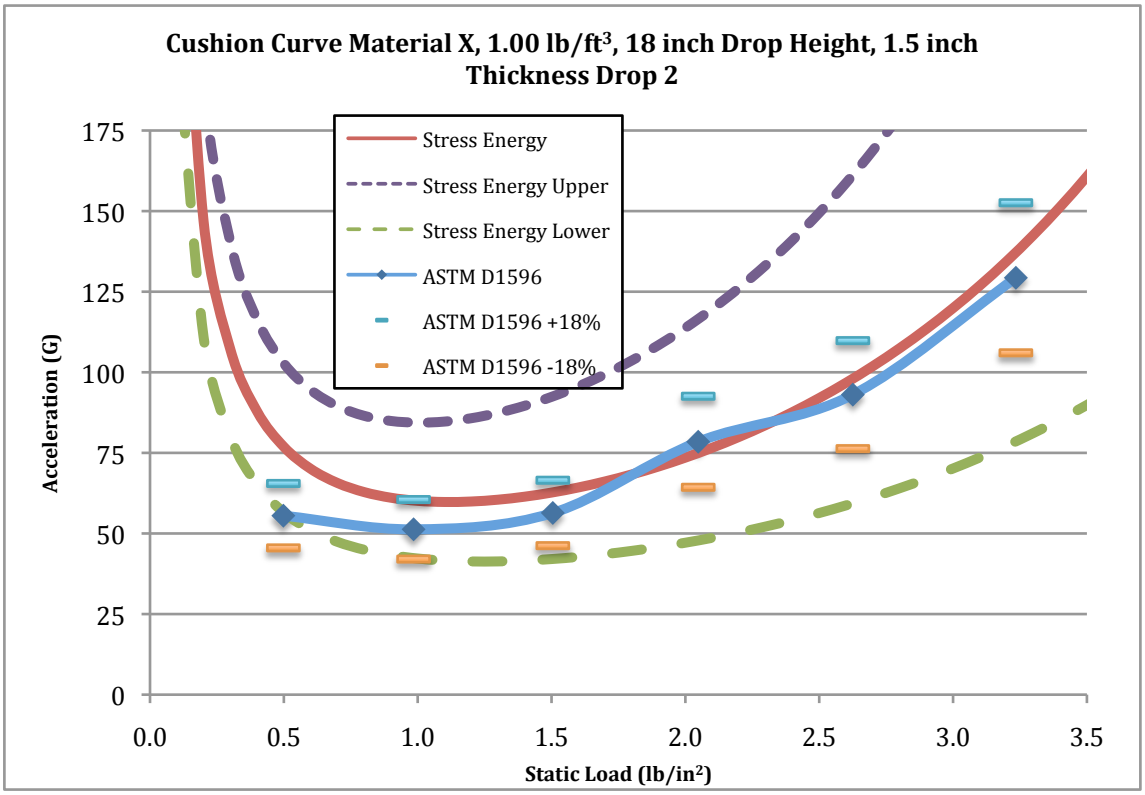

Figure 2: Predicted and Actual Cushion Curves, Confidence Bounds, ASTM Error Data Set A Drop 2

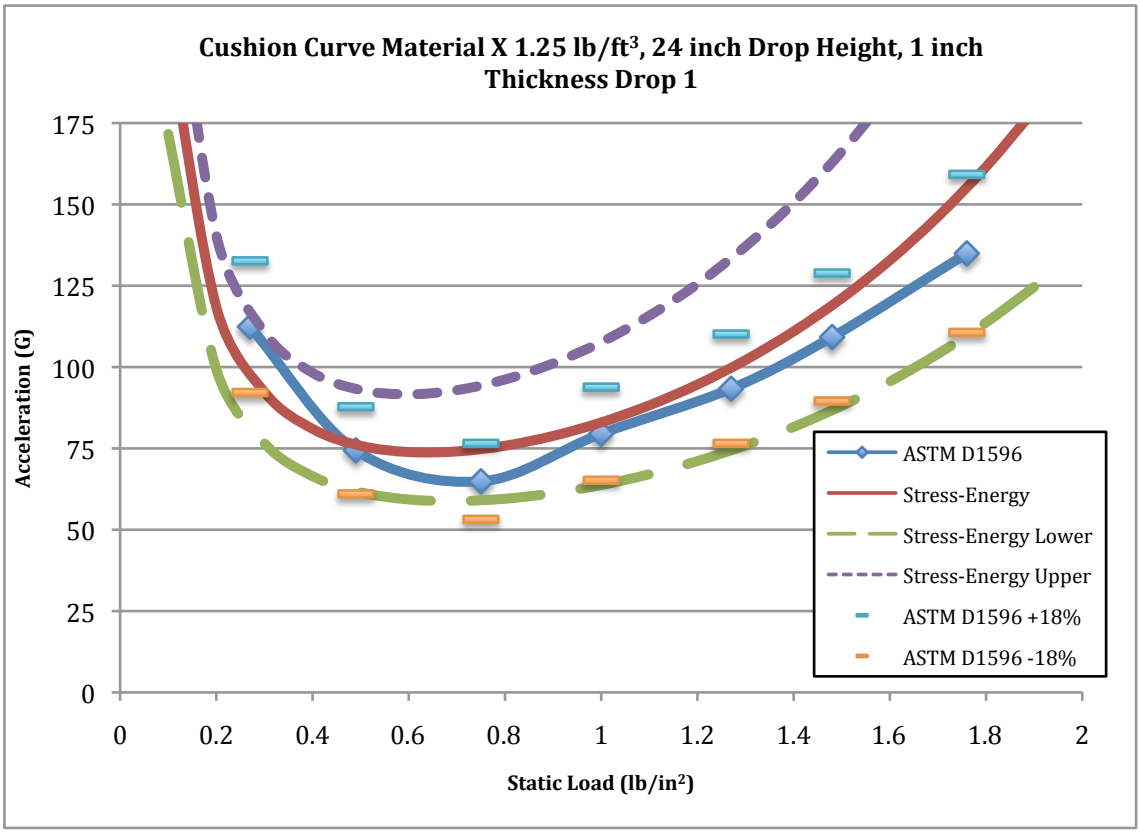

Figure 3: Predicted and Actual Cushion Curves, Confidence Bounds, ASTM Error Data Set B Drop 1

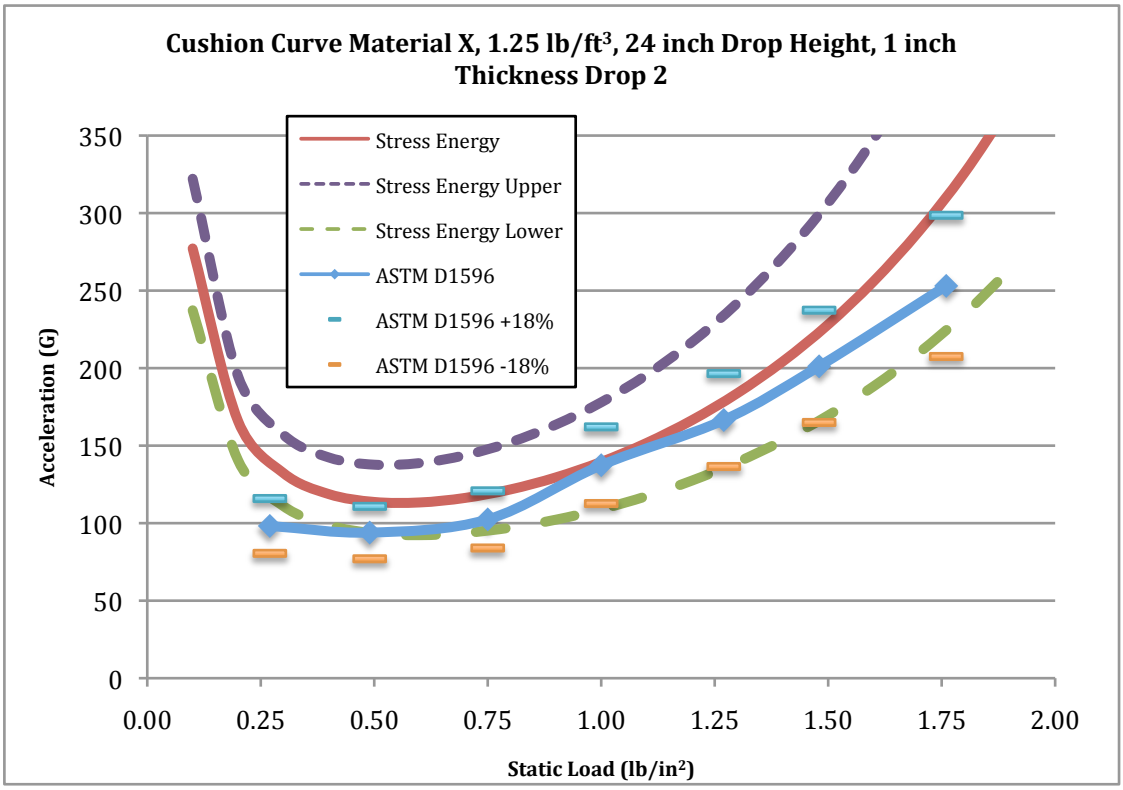

Figure 4: Predicted and Actual Cushion Curves, Confidence Bounds, ASTM Error Data Set B Drop 2

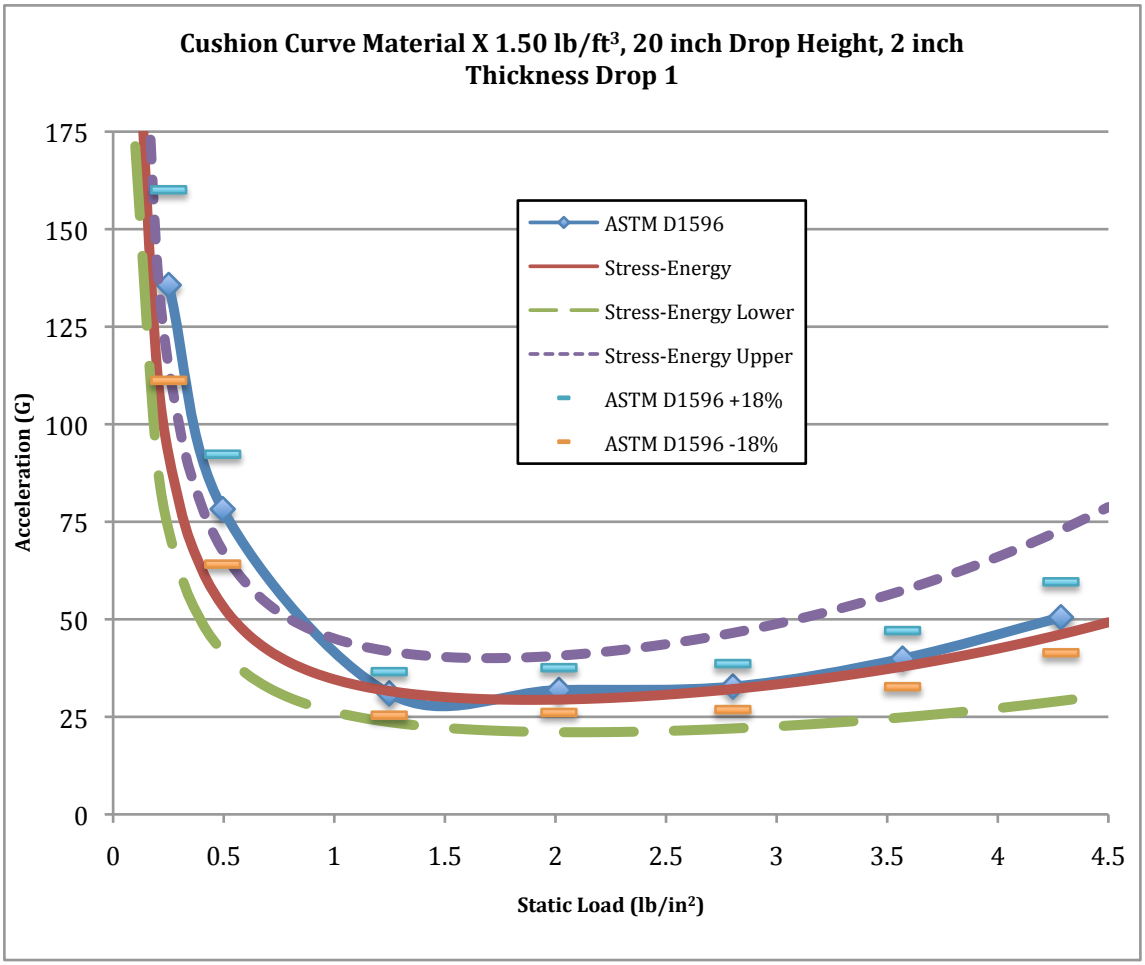

Figure 5: Predicted and Actual Cushion Curves, Confidence Bounds, ASTM Error Data Set C Drop 1

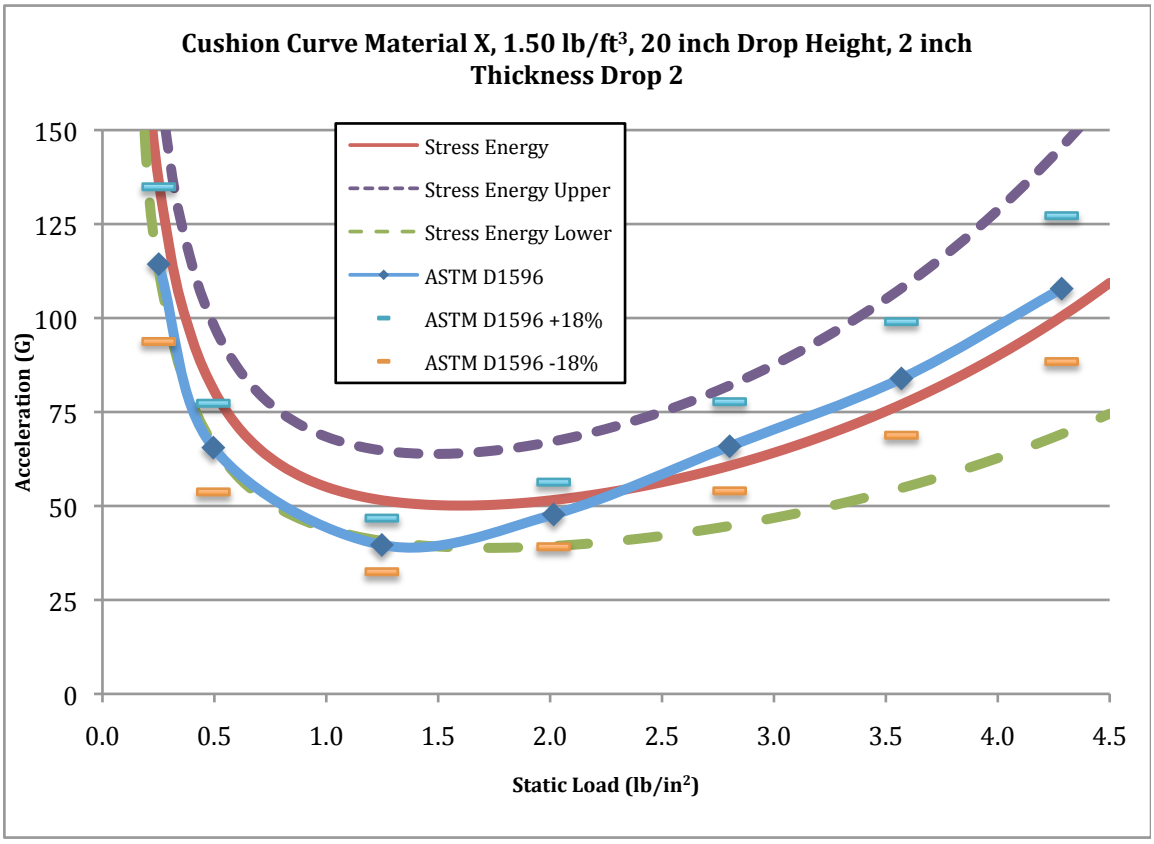

Figure 6: Predicted and Actual Cushion Curves, Confidence Bounds, ASTM Error Data Set C Drop 2

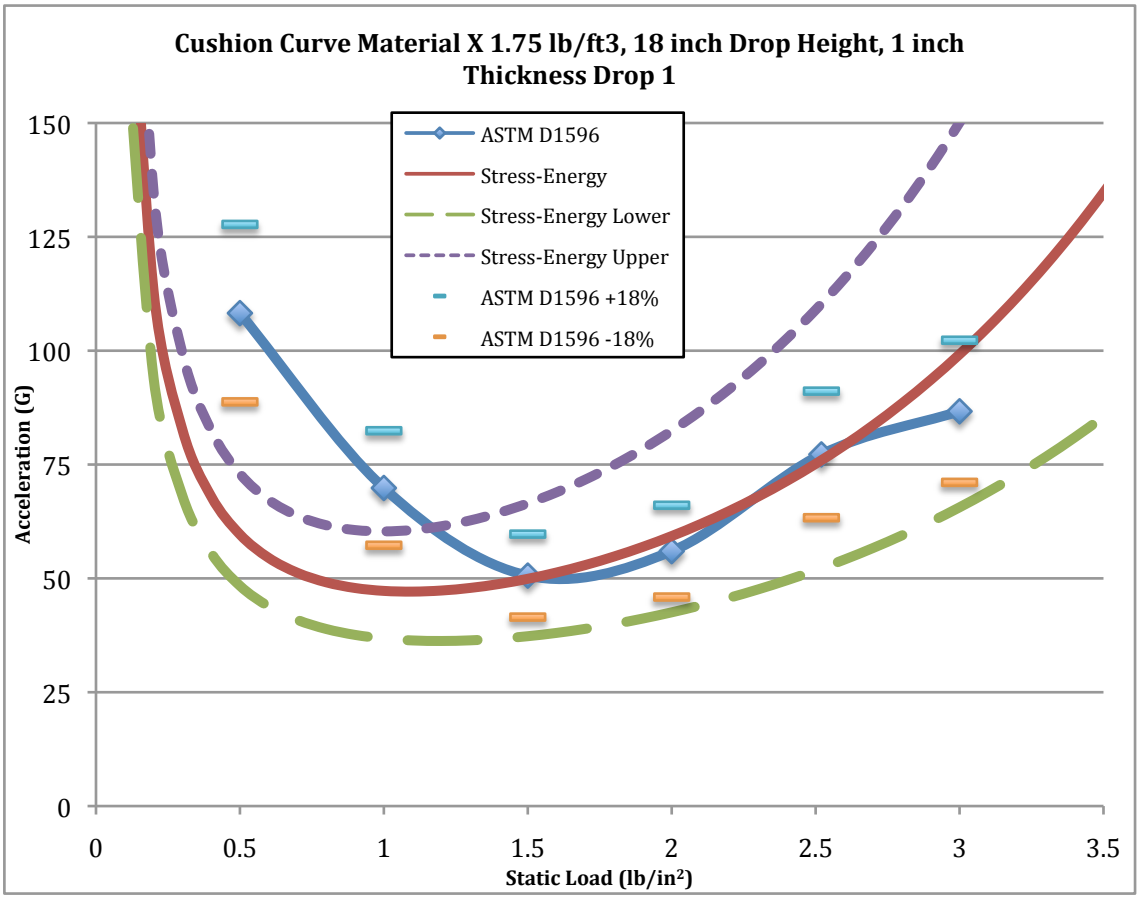

Figure 7: Predicted and Actual Cushion Curves, Confidence Bounds, ASTM Error Data Set D Drop 1

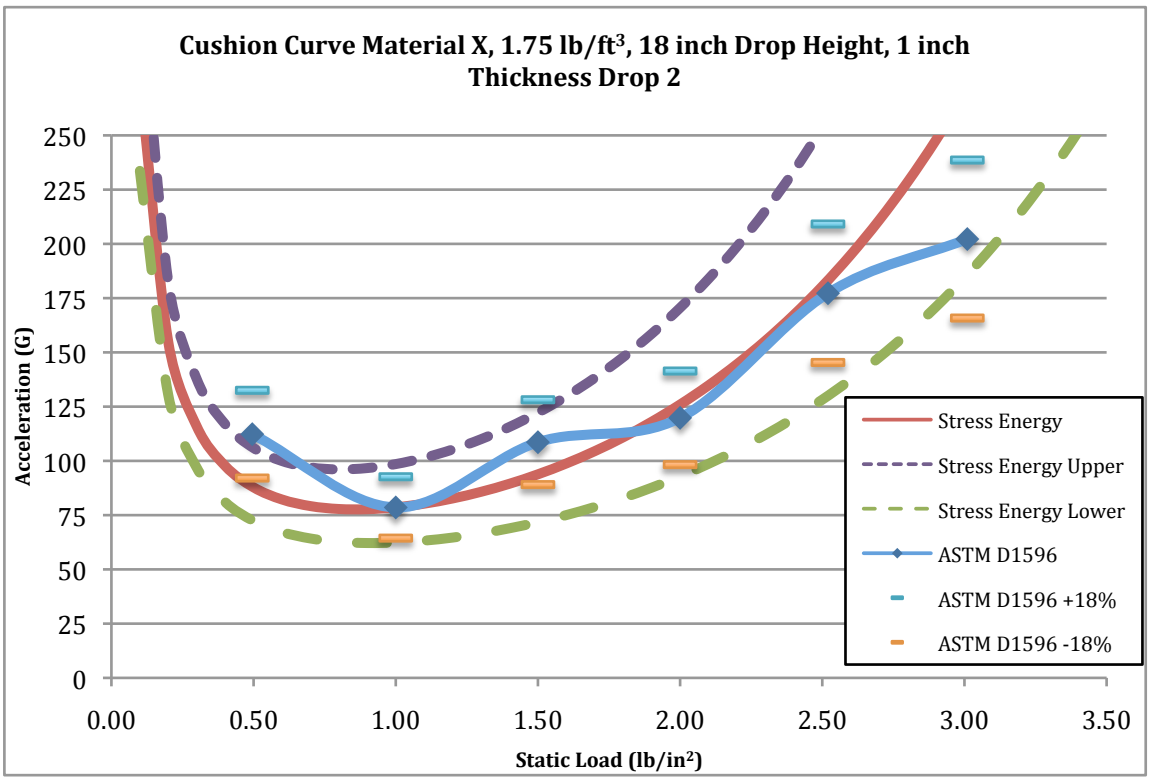

Figure 8: Predicted and Actual Cushion Curves, Confidence Bounds, ASTM Error Data Set D Drop 2

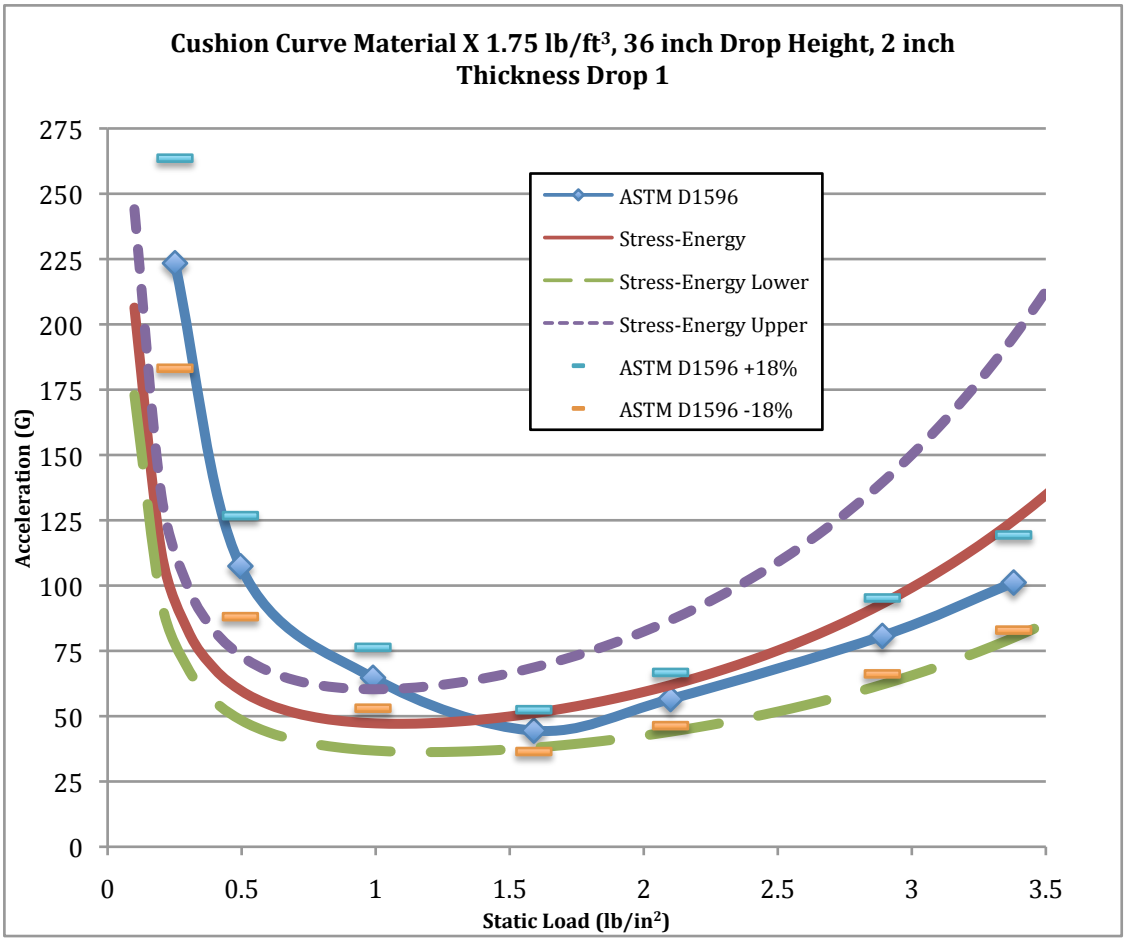

Figure 9: Predicted and Actual Cushion Curves, Confidence Bounds, ASTM Error Data Set E Drop 1

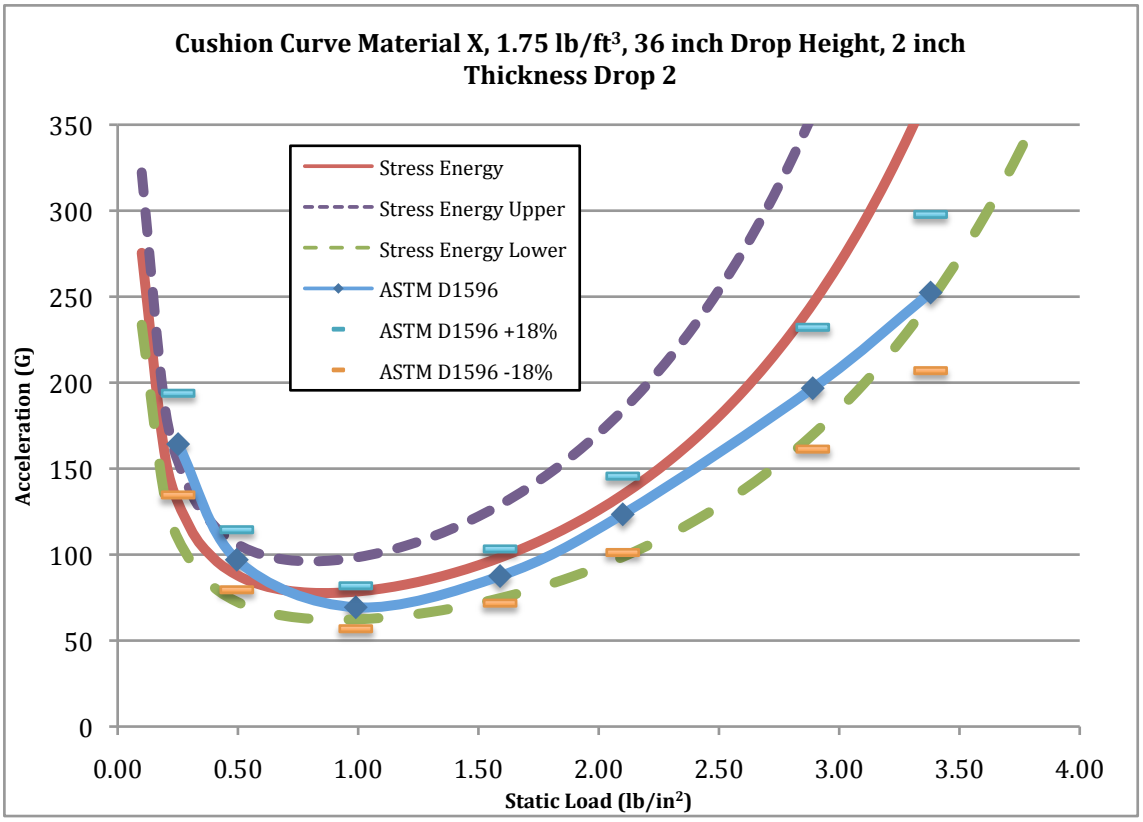

Figure 10: Predicted and Actual Cushion Curves, Confidence Bounds, ASTM Error Data Set E Drop 2

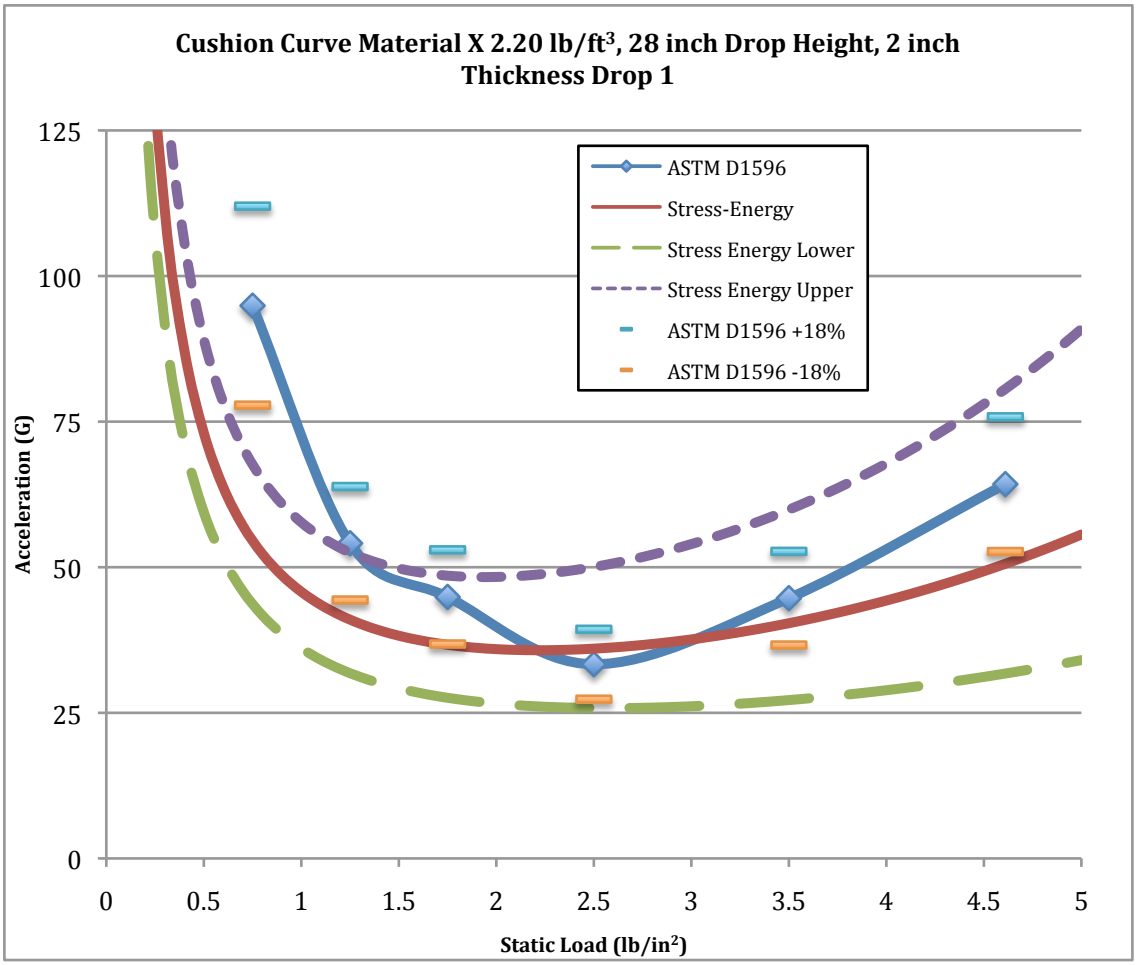

Figure 11: Predicted and Actual Cushion Curves, Confidence Bounds, ASTM Error Data Set F Drop 1

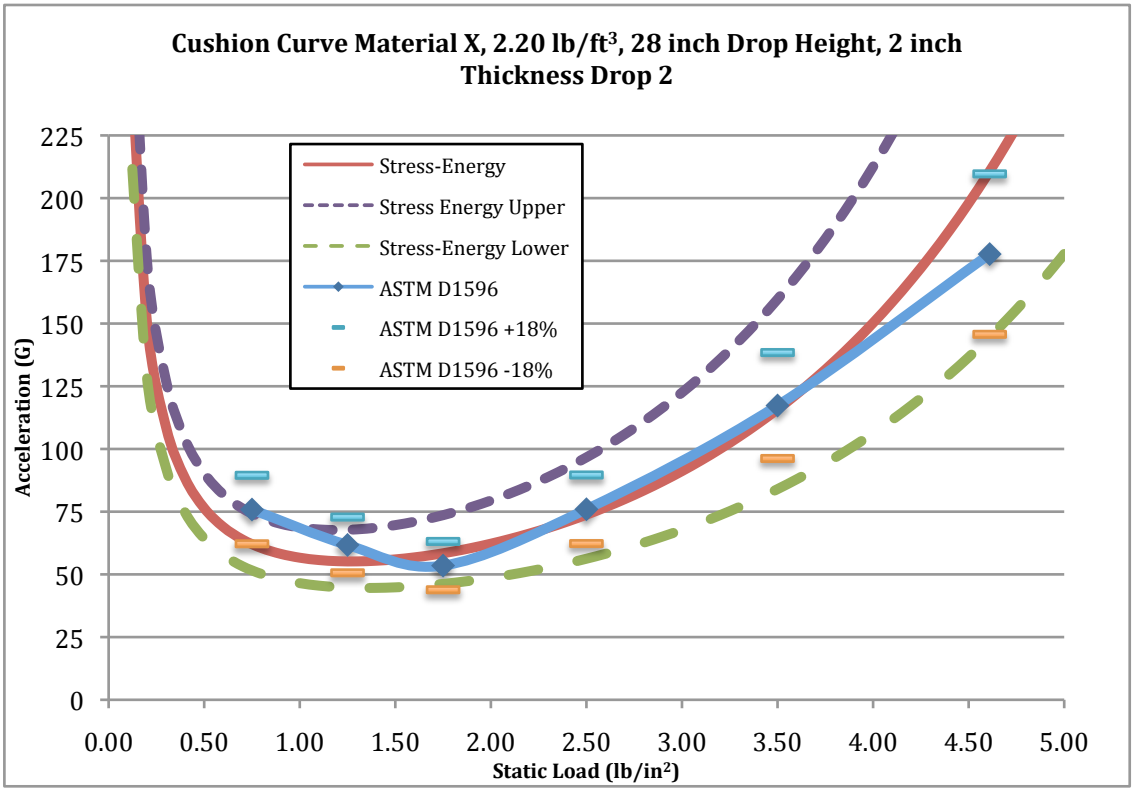

Figure 12: Predicted and Actual Cushion Curves, Confidence Bounds, ASTM Error Data Set F Drop 2

APPENDIX E:

Difference, percent difference and average percent difference between predicted and actual accelerations for Drop 1 and 2.

Table 1: Predicted and Actual Accelerations, Difference and Average Percent Difference Data Set A Drop 1

Static Load (lb/in^2)	Stress-Energy Predicted Acceleration (G's)	ASTM D1596 Acceleration (G's)	Difference (G's)	Percent Difference (%)	Average Percent Difference (%)
0.50	50.10	47.24	2.86	6.05	5.39
0.98	38.55	34.36	4.19	12.19	
1.50	39.3	38.22	1.08	2.83	
2.05	46.04	47.8	1.76	3.68	
2.63	58.96	57.81	1.15	1.99	
3.23	80.22	75.98	4.24	5.58	

Table 2: Predicted and Actual Accelerations, Difference and Average Percent Difference Data Set A Drop 2

Static Load (lb/in^2)	Stress-Energy Predicted Acceleration (G's)	ASTM D1596 Acceleration (G's)	Difference (G's)	Percent Difference (%)	Average Percent Difference (%)
0.50	77.03	55.52	21.51	38.75	13.89
0.98	60.23	51.29	8.94	17.42	
1.50	62.76	56.37	6.39	11.33	
2.05	74.96	78.45	3.49	4.45	
2.63	98.02	93.07	4.95	5.32	
3.23	137.18	129.32	7.86	6.08	

Table 3: Predicted and Actual Accelerations, Difference and Average Percent Difference Data Set B Drop 1

Static Load (lb/in^2)	Stress-Energy Predicted Acceleration (G's)	ASTM D1596 Acceleration (G's)	Difference (G's)	Percent Difference (%)	Average Percent Difference (%)
0.27	97.88	112.41	14.53	12.93	12.93
0.49	76.14	74.41	1.73	2.32	8.79
0.75	74.78	64.87	9.91	15.28	
1.00	82.99	79.52	3.47	4.36	
1.27	99.77	93.35	6.42	6.88	
1.48	118.98	109.24	9.74	8.92	
1.76	155.18	134.94	20.24	15.00	

Table 4: Predicted and Actual Accelerations, Difference and Average Percent Difference Data Set B Drop 2

Static Load (lb/in^2)	Stress-Energy Predicted Acceleration (G's)	ASTM D1596 Acceleration (G's)	Difference (G's)	Percent Difference (%)	Average Percent Difference (%)
0.27	139.29	98.20	41.09	41.84	41.84
0.49	113.93	93.93	20.00	21.30	13.21
0.75	118.71	102.42	16.30	15.91	
1.00	139.47	137.38	2.09	1.52	
1.27	178.32	166.52	11.80	7.09	
1.48	223.09	201.15	21.93	10.90	
1.76	310.13	253.04	57.08	22.56	

Table 5: Predicted and Actual Accelerations, Difference and Average Percent Difference Data Set C Drop 1

Static Load (lb/in^2)	Stress-Energy Predicted Acceleration (G's)	ASTM D1596 Acceleration (G's)	Difference (G's)	Percent Difference (%)	Average Percent Difference (%)
0.25	93.0	135.7	42.7	31.5	32.46
0.50	52.1	78.2	26.2	33.4	
1.25	31.6	31.0	0.6	2.0	5.03
2.02	29.4	31.9	2.4	7.6	
2.80	32.1	32.8	0.6	2.0	
3.57	37.9	39.9	2.0	5.1	
4.29	46.2	50.5	4.3	8.5	

Table 6: Predicted and Actual Accelerations, Difference and Average Percent Difference Data Set C Drop 2

Static Load (lb/in^2)	Stress-Energy Predicted Acceleration (G's)	ASTM D1596 Acceleration (G's)	Difference (G's)	Percent Difference (%)	Average Percent Difference (%)
0.25	137.8	114.3	23.4	20.5	21.7
0.50	80.6	65.5	15.0	22.9	
1.25	51.5	39.6	11.9	30.0	11.5
2.02	51.6	47.8	3.9	8.1	
2.80	60.7	65.9	5.2	7.9	
3.57	79.8	83.9	4.2	5.0	
4.29	100.6	107.8	7.2	6.7	

Table 7: Predicted and Actual Accelerations, Difference and Average Percent Difference Data Set D Drop 1

Static Load (lb/in^2)	Stress-Energy Predicted Acceleration (G's)	ASTM D1596 Acceleration (G's)	Difference (G's)	Percent Difference (%)	Average Percent Difference (%)
0.50	59.65	108.25	48.60	44.89	13.78
1.00	47.25	69.85	22.60	32.35	
1.50	49.91	50.61	0.70	1.39	
2.00	59.30	55.98	3.32	5.92	
2.52	75.94	77.22	1.28	1.66	
3.00	99.21	86.69	12.52	14.44	

Table 8: Predicted and Actual Accelerations, Difference and Average Percent Difference Data Set D Drop 2

Static Load (lb/in^2)	Stress-Energy Predicted Acceleration (G's)	ASTM D1596 Acceleration (G's)	Difference (G's)	Percent Difference (%)	Average Percent Difference (%)
0.50	88.14	112.31	24.17	21.52	13.00
1.00	78.60	78.55	0.05	0.06	
1.50	93.82	108.62	14.80	13.63	
2.00	125.98	119.84	6.14	5.12	
2.52	183.23	177.26	5.97	3.37	
3.01	271.48	202.23	69.25	34.24	

Table 9: Predicted and Actual Accelerations, Difference and Average Percent Difference Data Set E Drop 1

Static Load (lb/in^2)	Stress-Energy Predicted Acceleration (G's)	ASTM D1596 Acceleration (G's)	Difference (G's)	Percent Difference (%)	Average Percent Difference (%)
0.25	94.42	223.41	128.99	57.74	57.74
0.50	59.96	107.44	47.48	44.20	22.39
0.99	47.29	64.71	17.42	26.92	
1.59	51.15	44.48	6.67	14.98	
2.10	61.91	56.57	5.34	9.45	
2.89	93.07	80.73	12.34	15.29	
3.38	124.92	101.17	23.75	23.47	

Table 10: Predicted and Actual Accelerations, Difference and Average Percent Difference Data Set E Drop 2

Static Load (lb/in^2)	Stress-Energy Predicted Acceleration (G's)	ASTM D1596 Acceleration (G's)	Difference (G's)	Percent Difference (%)	Average Percent Difference (%)
0.25	130.76	164.27	33.51	20.40	20.40
0.50	88.14	97.01	8.87	9.14	19.35
0.99	78.47	69.38	9.09	13.11	
1.59	98.29	87.54	10.75	12.28	
2.10	134.80	123.44	11.36	9.21	
2.89	245.86	196.77	49.09	24.95	
3.38	372.03	252.41	119.62	47.39	

Table 11: Predicted and Actual Accelerations, Difference and Average Percent Difference Data Set F Drop 1

Static Load (lb/in^2)	Stress-Energy Predicted Acceleration (G's)	ASTM D1596 Acceleration (G's)	Difference (G's)	Percent Difference (%)	Average Percent Difference (%)
0.75	54.53	94.91	219.53	42.55	42.55
1.25	40.99	54.11	40.38	24.24	16.29
1.75	36.69	44.90	13.12	18.29	
2.50	36.02	33.34	8.21	8.04	
3.50	40.39	44.68	2.68	9.60	
4.61	50.59	64.26	4.29	21.27	

Table 12: Predicted and Actual Accelerations, Difference and Average Percent Difference Data Set F Drop 2

Static Load (lb/in^2)	Stress-Energy Predicted Acceleration (G's)	ASTM D1596 Acceleration (G's)	Difference (G's)	Percent Difference (%)	Average Percent Difference (%)
0.75	62.04	75.85	13.81	18.21	18.21
1.25	55.18	61.74	6.56	10.63	8.51
1.75	58.42	53.5	4.92	9.20	
2.50	73.81	75.96	2.15	2.83	
3.50	115.84	117.32	1.48	1.26	
4.61	210.73	177.69	33.04	18.60	

APPENDIX F:

Between lab acceleration error allowed by ASTM D1596 for Drop 1 and 2. An asterisk (*) represents a static load not typically chosen for energy absorbing applications.

Table 1: Between Lab Acceleration Error Data Set A Drop 1

Static Load (lb/in^2)	Stress-Energy Predicted Acceleration (G's)	ASTM D1596 Acceleration (G's)	+18% Error (G's)	-18% Error (G's)	Did Predicted Fall Within Error?	Missed Closest Limit By (G's)
0.50	50.10	47.24	55.74	38.74	yes	-
0.98	38.55	34.36	40.54	28.18	yes	-
1.50	39.3	38.22	45.10	31.34	yes	-
2.05	46.04	47.8	56.40	39.20	yes	-
2.63	58.96	57.81	68.22	47.40	yes	-
3.23	80.22	75.98	89.66	62.30	yes	-

Table 2: Between Lab Acceleration Error Data Set A Drop 2

Static Load (lb/in^2)	Stress-Energy Predicted Acceleration (G's)	ASTM D1596 Acceleration (G's)	+18% Error (G's)	-18% Error (G's)	Did Predicted Fall Within Error?	Missed Closest Limit By (G's)
0.50	77.03	55.52	65.51	45.53	no	11.52
0.98	60.23	51.29	60.52	42.06	yes	-
1.50	62.76	56.37	66.52	46.22	yes	-
2.05	74.96	78.45	92.57	64.33	yes	-
2.63	98.02	93.07	109.82	76.32	yes	-
3.23	137.18	129.32	152.60	106.04	yes	-

Table 3: Between Lab Acceleration Error Data Set B Drop 1

Static Load (lb/in^2)	Stress-Energy Predicted Acceleration (G's)	ASTM D1596 Acceleration (G's)	+18% Error (G's)	-18% Error (G's)	Did Predicted Fall Within Error?	Missed Closest Limit By (G's)
0.27*	97.88	112.41	132.6	92.2	yes	-
0.49	76.14	74.41	87.8	61.0	yes	-
0.75	74.78	64.87	76.5	53.2	yes	-
1.00	82.99	79.52	93.8	65.2	yes	-
1.27	99.77	93.35	110.2	76.5	yes	-
1.48	118.98	109.24	128.9	89.6	yes	-
1.76	155.18	134.94	159.2	110.7	yes	-

Table 4: Between Lab Acceleration Error Data Set B Drop 2

Static Load (lb/in^2)	Stress-Energy Predicted Acceleration (G's)	ASTM D1596 Acceleration (G's)	+18% Error (G's)	-18% Error (G's)	Did Predicted Fall Within Error?	Missed Closest Limit By (G's)
0.27*	139.29	98.20	115.88	80.53	no	23.41
0.49	113.93	93.926	110.83	77.02	no	3.10
0.75	118.71	102.42	120.85	83.98	yes	
1.00	139.47	137.38	162.11	112.65	yes	
1.27	178.32	166.52	196.49	136.54	yes	
1.48	223.09	201.15	237.36	164.95	yes	
1.76	310.13	253.04	298.59	207.50	no	11.54

Table 5: Between Lab Acceleration Error Data Set C Drop 1

Static Load (lb/in^2)	Stress-Energy Predicted Acceleration (G's)	ASTM D1596 Acceleration (G's)	+18% Error (G's)	-18% Error (G's)	Did Predicted Fall Within Error?	Missed Closest Limit By (G's)
0.25*	92.96	135.68	160.10	111.25	no	18.29
0.50*	52.07	78.23	92.31	64.15	no	12.08
1.25	31.60	31.00	36.58	25.42	yes	-
2.02	29.43	31.86	37.60	26.13	yes	-
2.80	32.11	32.75	38.65	26.86	yes	-
3.57	37.89	39.92	47.10	32.73	yes	-
4.29	46.20	50.51	59.61	41.42	yes	-

Table 6: Between Lab Acceleration Error Data Set C Drop 2

Static Load (lb/in^2)	Stress-Energy Predicted Acceleration (G's)	ASTM D1596 Acceleration (G's)	+18% Error (G's)	-18% Error (G's)	Did Predicted Fall Within Error?	Missed Closest Limit By (G's)
0.25*	137.18	114.33	134.91	93.75	no	2.27
0.50*	81.07	65.53	77.33	53.73	no	3.75
1.25	51.53	39.634	46.77	32.50	no	4.76
2.02	51.58	47.746	56.34	39.15	yes	-
2.80	60.70	65.88	77.74	54.02	yes	-
3.57	77.02	83.926	99.03	68.82	yes	-
4.29	100.41	107.82	127.23	88.41	yes	-

Table 7: Between Lab Acceleration Error Data Set D Drop 1

Static Load (lb/in^2)	Stress-Energy Predicted Acceleration (G's)	ASTM D1596 Acceleration (G's)	+18% Error (G's)	-18% Error (G's)	Did Predicted Fall Within Error?	Missed Closest Limit By (G's)
0.50	59.65	108.25	127.74	88.77	no	29.11
1.00	47.25	69.85	82.42	57.28	no	10.02
1.50	49.91	50.61	59.72	41.50	yes	-
2.00	59.30	55.98	66.06	45.90	yes	-
2.52	75.94	77.22	91.12	63.32	yes	-
3.00	99.21	86.69	102.29	71.09	yes	-

Table 8: Between Lab Acceleration Error Data Set D Drop 2

Static Load (lb/in^2)	Stress-Energy Predicted Acceleration (G's)	ASTM D1596 Acceleration (G's)	+18% Error (G's)	-18% Error (G's)	Did Predicted Fall Within Error?	Missed Closest Limit By (G's)
0.50	88.14	112.31	132.53	92.09	no	3.95
1.00	78.60	78.55	92.69	64.41	yes	-
1.50	93.82	108.62	128.17	89.07	yes	-
2.00	125.98	119.84	141.41	98.27	yes	-
2.52	183.23	177.26	209.17	145.35	yes	-
3.01	271.48	202.23	238.63	165.83	no	32.85

Table 9: Between Lab Acceleration Error Data Set E Drop 1

Static Load (lb/in^2)	Stress-Energy Predicted Acceleration (G's)	ASTM D1596 Acceleration (G's)	+18% Error (G's)	-18% Error (G's)	Did Predicted Fall Within Error?	Missed Closest Limit By (G's)
0.25*	94.42	223.41	263.62	183.20	no	88.78
0.50	59.96	107.44	126.78	88.10	no	28.14
0.99	47.29	64.71	76.36	53.06	no	5.77
1.59	51.15	44.48	52.49	36.47	yes	-
2.10	61.91	56.57	66.75	46.39	yes	-
2.89	93.07	80.73	95.26	66.20	yes	-
3.38	124.92	101.17	119.38	82.96	no	5.53

Table 10: Between Lab Acceleration Error Data Set E Drop 2

Static Load (lb/in^2)	Stress-Energy Predicted Acceleration (G's)	ASTM D1596 Acceleration (G's)	+18% Error (G's)	-18% Error (G's)	Did Predicted Fall Within Error?	Missed Closest Limit By (G's)
0.25*	130.76	164.27	193.84	134.70	no	3.94
0.50	88.14	97.01	114.47	79.55	yes	
0.99	78.47	69.38	81.87	56.89	yes	
1.59	98.29	87.54	103.30	71.78	yes	
2.10	134.80	123.44	145.66	101.22	yes	
2.89	245.86	196.77	232.19	161.35	no	13.68
3.38	372.03	252.41	297.84	206.98	no	74.18

Table 11: Between Lab Acceleration Error Data Set F Drop 1

Static Load (lb/in^2)	Stress-Energy Predicted Acceleration (G's)	ASTM D1596 Acceleration (G's)	+18% Error (G's)	-18% Error (G's)	Did Predicted Fall Within Error?	Missed Closest Limit By (G's)
0.75*	54.53	94.91	111.99	77.83	no	23.30
1.25	40.99	54.11	63.85	44.37	no	3.38
1.75	36.69	44.90	52.98	36.82	yes	-
2.50	36.02	33.34	39.34	27.34	yes	-
3.50	40.39	44.68	52.72	36.64	yes	-
4.61	50.59	64.26	75.83	52.69	no	2.10

Table 12: Between Lab Acceleration Error Data Set F Drop 2

Static Load (lb/in^2)	Stress-Energy Predicted Acceleration (G's)	ASTM D1596 Acceleration (G's)	+18% Error (G's)	-18% Error (G's)	Did Predicted Fall Within Error?	Missed Closest Limit By (G's)
0.75*	62.04	75.85	89.50	62.20	no	0.16
1.25	55.18	61.74	72.85	50.63	yes	-
1.75	58.42	53.5	63.13	43.87	yes	-
2.50	73.81	75.96	89.63	62.29	yes	-
3.50	115.84	117.32	138.44	96.20	yes	-
4.61	210.73	177.69	209.67	145.71	no	1.06

REFERENCES:

ASTM D1596-97(2011), "Standard Test Method for Dynamic Shock Cushioning Characteristics of Packaging Material," ASTM International, West Conshohocken, PA. DOI: 10.1520/D1596-97RO3, www.astm.org.

Burgess, G. (1990). Consolidation of Cushion Curves. Packaging Technology and Science, 3, 189-194.

Daum, M. (2006). "A simplified process for determining cushion curves: The stress-energy method". Proceedings from Dimensions 2006. San Antonio, TX.

Daum, M. (2011). "Stress-Energy vs. ASTM D1596." Journal of Testing and Evaluation. Vol. 39, No. 6.

Hanlon, Joseph. Kelsey, Robert. Forcinio, Hallie. (1998). Handbook of Package Engineering. Third Edition. Lancaster, Pennsylvania: Technomic Publishing Company, Inc.

Klempner, Daniel. Sendijarevic, Vahid. Aseeva, Roza. (2004). Handbook of Polymeric Foams and Foam Technology. Cincinnati, Ohio: Hanser Gardner Publications, Inc.

Lee, S. Park, C. Ramesh, N. (2007). Polymeric Foams Science and Technology. Boca Raton, Florida: CRC Press.

Marcondes, P., Batt, G., Darby, D., and Daum, M. (2008). "Minimum Samples Needed to Construct Cushion Curves Based on the Stress Energy Method". Journal of Applied Packaging Research. Vol. 2, No. 3. 191-198.

Nova Chemicals. (2007). Cushion Curve 1.3 pcf. ARCEL Advanced Foam Resin. March 1, 2012. http://www.novachem.com/ARCEL/docs/CushionCurves/Cushion_1.3_pcf_.pdf.

Rabenhorst, Randy. (2006). "Cushion Specification: Impact of MADE Study Data on Cushion Design." Dimensions.06 International Conference on Transport Packaging, San Antonio, TX.

Potter, Glen A. "Performance of Expanded Polymer Cushion Materials At Less Than One Inch Thick." Thesis. Clemson University, 2010. *Electronic Thesis and Dissertations*. Clemson Library, May 2010. Feb. 2011. http://etd.lib.clemson.edu/documents/1285777090/.

Singh L. Ignatova E, Olsen, P Singh. (2010). "Evaluation of Stress-Energy Methodology to Predict Transmitted Shock Through Expanded Foam Cushion." Journal of Testing and Evaluation; vol 38: n6: 1-7.

Soroka, Walter. (2002). Fundamentals of Packaging Technology. Naperville, Illinois: Institute of Packaging Professionals.